Supporting Information

Tailoring the Electron-Deficient Central Core on Fused-Ring Nonfullerene Acceptors: Deciphering The Relationships Between Structure, Property, And Photovoltaic Performance

Fátima Suárez-Blas, Lorenzo Pandolfi, Matías J. Alonso-Navarro, Sergi Riera-Galindo, José Ignacio Martínez, Bernhard Dörling, Alejandro Funes, Albert Harillo, Elisabetta Venuti, M. Mar Ramos, Mariano Campoy-Quiles, José L. Segura**

Table of contents

1. General Information.

All the chemicals were purchased from commercial suppliers and used without further purification. Compounds **BTD-2TTP**, **NID** and **PID** were obtained as previously described or with some modifications.[1] ^{1}H-NMR and ^{13}C-NMR spectra were recorded on a Bruker Avance 300 MHz and AMX 500 spectrometers. Chemical shifts are reported in ppm and referenced to the residual non-deuterated solvent frequencies ($CDCl_3$: δ 7.26 ppm for ^{1}H, δ 77.0 ppm for ^{13}C). UV-Vis absorption spectra of the compounds in HPLC chloroform solutions at 20 ºC were recorded on a Varian Cary 50 UV-Vis spectrophotometer and fluorescence spectra were recorded on a Perkin-Elmer LS 55 fluorescence spectrometer. Mass spectra were recorded on a Bruker Reflex 2 (MALDI-TOF). FTIR spectra were carried out in a Shimadzu FTIR 8300 spectrophotometer. Cyclic voltammograms were recorded in an inert atmosphere in electrochemical workstation at a scan rate of 100 $mV \cdot s^{-1}$ at 20 ºC using tetrabutylammonium hexafluorophosphate (TBAHFP, 0.1 $mol \cdot L^{-1}$) as supporting electrolyte in dichloromethane. Polymer-precoated platinum electrode, platinum-wire electrode, and Ag/Ag^{+} electrode were used as working electrode, an auxiliary electrode, and reference electrode, respectively. Potentials were recorded versus Fc/Fc^{+}.

Thin-film samples for Raman, PL and Ellipsometry. Solutions of **Y6**, **Y6-1Napht** and **Y6-1Pery** were prepared by mixing ≈ 5 mg of synthetized powder with 250 µL of chlorobenzene (c ≈ 20 mg/mL) in a nitrogen-filled glove box. The solutions were stirred for 2 hours. Glass substrates were cleaned by ultra-sonication in acetone (5 min), followed by a 10 % Hellmanex solution (aq.) (5 min), isopropanol (5 min) and NaOH 10 % (aq.) (10 min). Subsequently, ≈ 60 µL of solution were deposited by blade coating (ZUA 2000, Zehntner), with a blade gap of 100 µm, at 80 °C to enhance the rapid evaporation of the solvent. For the samples with thermal gradient, also inside the glovebox, a thermal annealing was applied with a Kofler bench (Lab Logistics Group GmbH), which exhibits a thermal gradient of ≈ 8 °C/cm, with a temperature range extending from 30 °C to more than 250 °C. Three adjacent glass slides were annealed for 10 min, covering a range of temperatures from 70 °C to 250 °C.

Computational methods. Density functional calculations were carried out utilizing the B3LYP functional[2] and the 6-311G** basis set[3] as implemented in the Gaussian16 atomistic simulation package.[4] Time-dependent DFT (TDDFT) calculations[5] at the B3LYP/6-311G** level of theory were subsequently conducted on the optimized geometries to gain insights into their absorption spectra. For all structures under examination, the twenty lowest-energy electronic excited states were computed. The internal reorganization energies for both electron and hole transport in this semiconductor series

were determined following previously described methods.[6] The intramolecular reorganization energy, a parameter reflecting the structural adjustments necessary to accommodate added charge, was computed, with an emphasis on achieving small reorganization energies as a prerequisite for efficient charge transport.

Raman and PL measurements. Raman spectra were collected on the not annealed thin-film samples, using a WITec alpha 300 RA+ confocal Raman setup coupled with an Olympus objective with 100× magnification and a 488 nm laser line as excitation wavelength. A 785 nm laser line was chosen as excitation wavelength for photoluminescence measurements, based on the studies of absorption spectroscopy on these systems.

Ellipsometry. Variable angle spectroscopic ellipsometry (VASE) was measured using a Semilab GES5E rotating polarizer ellipsometer. The ellipsometric angles were recorded for a minimum of three incidence angles. Modeling of the ellipsometry data was performed using the Winelli II piece of software package from SOPRALAB using the standard critical point model for the dielectric function of the different materials.

Organic solar cells. All devices were manufactured with an inverted architecture (glass/ITO/ZnO/PAL/MoO_3/Ag). The thin films for the fabrication of organic solar cells were obtained by the same meniscus-shearing technique described above. ITO substrates (purchased from Ossila) were cleaned as described above for thin film sample preparation, and subsequently coated with ZnO nanoparticle dispersions (N-10, Avantama) onto the ITO-substrates at 40 °C, with a coating speed of 5 mm/s and blade gap of 50 µm. A thermal annealing at 100 °C for about 10 minutes was applied. Then, the samples were transferred into a nitrogen filled glove box. The active layer of acceptor:donor solutions (**Y6-derivative:PM6**) with w/w ratio of 1.6:1 (concentration of ≈ 15 mg/mL in chloroform) was blade coated at an accelerated speed in order to generate a thickness gradient. The blade gap was 100 µm and the substrate temperature was 40 °C. 24 pixels (12 at each side) where defined by evaporating MoO_x and Ag as top electrode through a shadow mask. Each of the 12 pixels exhibited a different active layer thickness. The J–V measurements were automatically acquired in ambient conditions using a Keithley 2400 source meter in combination with an Arduino-based multiplexer/switcher that allows data collection of up to 24 devices in a row. A SAN-EI Electric, XES-100S1 AAA solar simulator was used as

AM1.5G illumination source. The solar simulator was previously calibrated with a certified silicon solar cell (NREL).

2. Synthesis of compounds and characterization.

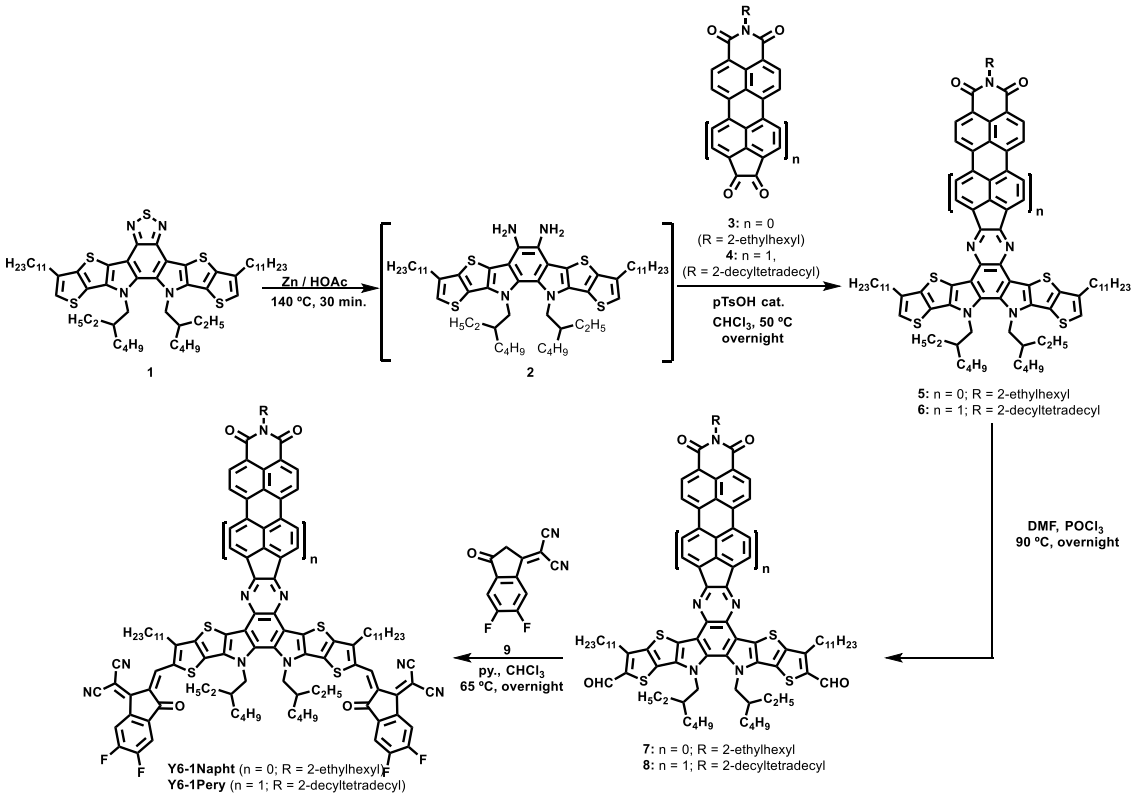

Scheme S1. Synthetic route for Y6-1Napht and Y6-1Pery.

NIP-2TTP (5)

Under Ar atmosphere, **BTD-2TTP (1)** (300 mg, 0.31 mmol) is suspended in 15 mL of acetic acid and heated at 140 ºC until everything is dissolved. Zn powder is added (262 mg, 4 mmol) and the mixture is stirring 30 min. After that, this solution was added to another solution containing **NID (3)** (112 mg, 0.31 mmol) and a catalytic amount of *p*-TsOH (10%), dissolved in 15 mL of anhydrous chloroform under Ar

atmosphere. Then, the reaction mixture was heated at 50 ºC and stirred at this temperature for 24 h. Once the reaction was cooled down, the solvent was half-reduced under reduced pressure, and then precipitated with MeOH. After washing with cold and hot methanol, **NIP-2TTP (5)** was obtained as a brown powder (298 mg, 76%).

^{1}H-NMR (300 MHz, $CDCl_3$): δ (ppm) = 8.64 (d, J = 7.3 Hz, 2H), 8.53 (d, J = 7.3 Hz, 2H), 7.06 (s, 2H), 4.68 (m, 4H), 4.15 (m, 2H), 2.90-2.83 (m, 4H), 2.14 (m, 2H), 1.93 (m, 4H), 1.45-1.29 (m, 39H), 1.18 – 0.91 (m, 30H), 0.73 – 0.59 (m, 12H).

^{13}C-NMR (75 MHz, $CDCl_3$): δ (ppm) = 164.34, 151.26, 143.76, 138.96, 138.30, 137.09, 132.66, 131.11, 123.84, 123.68, 122.19, 121.77, 119.54, 119.46, 119.13, 55.12, 40.09, 38.43, 32.08, 30.98, 29.88, 29.83, 29.68, 29.53, 29.05, 27.87, 23.29, 22.95, 22.85, 14.28, 13.91, 10.86, 10.28.

FTIR (ATR, $CHCl_3$): υ (cm^{-1}): 2961, 2927, 2850, 2354, 1702, 1665, 1564, 1521, 1465, 1381, 1324, 1258, 1236, 1166, 1085, 1016, 809, 753, 716.

MALDI-HRMS (*m*/*z*:): calculated for $C_{78}H_{103}N_5O_2S_4$: 1269.6995, found (M^+): 1629.6941.

NIP-2TTP-DIA (7)

Under Ar atmosphere, **NID-2TTP (5)** (149 mg, 0.12 mmol) is suspended in 5 mL of dry DMF And cooled down to 0 °C and $POCl_3$ (0,33 mL, 3.5 mmol) was added. Then, the reaction mixture was stirred at 0 °C for 2h and, after that time, heated to 90 ºC overnight. Once the time is over, the reaction was cooled, and the crude was poured into NaOH 4M solution and extracted with dichloromethane (3 times). The combined organic phases were dried over $MgSO_4$ and, after removal of the solvent, purified by column chromatography in dichloromethane/hexane 1:1, to give **NIP-2TTP-DIA (7)** as a brown solid (135 mg, 68%).

^{1}H-NMR (300 MHz, $CDCl_3$): δ (ppm) = 10.17 (s, 2H), 8.67 (d, J = 7.2 Hz, 2H), 8.56 (d, J =7.2 Hz, 2H), 4.72 (m, 4H), 4.16 (m, 2H), 3.31-3.20 (m, 4H), 2.18-2.08 (m, 2H), 2.00-1.94 (m, 4H), 1.40-1.20 (m, 39H), 1.08 – 0.82 (m, 30H), 0.71 (td, J = 7.4, 2.7 Hz, 6H), 0.63 (td, J = 7.3, 2.0 Hz, 6H).

^{13}C-NMR (75 MHz, $CDCl_3$): δ (ppm) = 182.02, 164.12, 152.05, 147.05, 144.69, 138.18, 137.88, 137.24, 134.37, 133.42, 132.62, 132.05, 129.67, 126.63, 125.38, 124.27, 122.60, 119.65, 55.31, 40.31, 38.44,

32.05, 30.74, 29.82, 29.72, 29.61, 29.49, 28.93, 28.33, 27.77, 27.74, 23.28, 22.92, 22.83, 14.31, 14.26, 13.87, 10.85, 10.37, 10.33.

FTIR (ATR, $CHCl_3$): υ (cm–1): 2962, 2927, 2853, 2726, 2355, 1704, 1658, 1559, 1513, 1464, 1414, 1329, 1233, 1167, 1095, 856, 820, 751.

MALDI-HRMS (*m/z*): calculated for $C_{80}H_{103}N_5O_4S_4$: 1325.6893, found (M^+): 1325.6836.

Y6-1Napht

Under Ar atmosphere, **NIP-2TTP-DIA (7)** (56 mg, 0.04 mmol) and 2-(3-oxo-2,3-dihydro-1H-inden-1-ylidene)malononitrile **9** (40.8 mg, 0.18 mmol) are suspended in 5 mL of dry chloroform and heated at 65 ºC until everything was dissolved. Then, pyridine (0.05 mL, 0.63 mmol) was added and the reaction was stirred at 65 ºC overnight. Once the reaction time was over, the reaction was cooled and the solvent was removed under reduced pressure and the residue was purified by column chromatography in dichloromethane/hexane 5:1, to give the product **Y6-1Napht** as a blue solid (58 mg, 54%).

^{1}H-NMR (300 MHz, $CDCl_3$): δ (ppm) = 9.03 (s, 2H), 8.48 (d, J = 7.2 Hz, 2H), 8.41 (dd, J= 9, 6 Hz, 2H), 8.22 (d, J = 7.2 Hz, 2H), 7.70 (t, J = 7.5 Hz, 2H), 4.93-4.82 (m, 4H), 4.23-4.14 (m, 2H), 3.29-3.18 (m, 4H), 2.31-2.21 (m, 2H), 1.93-1.85 (m, 3H), 1.37-1.18 (m, 52H), 0.87-0.68 (m, 30H).

^{13}C-NMR (175 MHz, $CDCl_3$): δ (ppm) = 186.34, 163.97, 158.90, 154.14, 152.51, 146.66, 138.78, 137.59, 136.78, 136.07, 135.46, 134.72, 134.64, 134.59, 133.45, 133.40, 133.00, 132.60, 130.26, 129.88, 125.33, 124.52, 122.87, 120.69, 120.02, 115.14, 115.11, 114.69, 112.71.

FTIR (ATR, $CHCl_3$): υ (cm^{-1}): 2965, 2927, 2855, 2358, 2217, 1706, 1670, 1536, 1431, 1369, 1349, 1294, 1232, 1199, 1150, 1105, 893, 777.

MALDI-HRMS (*m/z*): calculated for $C_{104}H_{107}F_4N_9O_4S_4$: 1749.7265, found ($M^+$): 1749.7259.

PIP-2TTP (6)

Under Ar atmosphere, **BTD-2TTP (1)** (40 mg, 0.04 mmol) is suspended in 2 mL of acetic acid and heated at 140 ºC until everything is dissolved. Zn powder is added (40 mg, 0.62 mmol) and the mixture is stirring 30 min. After that, this solution was added to another solution containing **PID (4)** (30 mg, 0.04 mmol) and a catalytic amount of *p*-TsOH (10%), dissolved in 2 mL of anhydrous chloroform under Ar

atmosphere. Then, the reaction mixture was heated at 50 ºC and stirred at this temperature for 24 h. Once the reaction was cooled down, the solvent was half-reduced under reduced pressure, and then precipitated with MeOH. After washing with cold and hot methanol, **PIP-2TTP (6)** was obtained as a brown powder (40 mg, 60%).

^{1}H-NMR (300 MHz, $CDCl_3$): δ (ppm) = 8.27 (d, J = 8.0 Hz, 2H), 8.15-8.07 (m, 4H), 7.91-7.99 (m, 2H), 6.93 (s, 2H), 4.81-4.67 (m, 4H), 3.84-3.75 (m, 2H), 2.75-2.68 (m, 4H), 2.41-2.28 (m, 2H), 1.91-1.78 (m, 5H), 1.37-1.22 (m, 76H), 0.97-0.63 (m, 36H).

^{13}C-NMR (75 MHz, $CDCl_3$): δ (ppm) = 163.66, 157.58, 149.73, 143.69, 137.76, 136.90, 135.16, 134.72, 133.90, 133.00, 132.99, 130.77, 130.52, 129.66, 129.58, 129.49, 126.21, 123.19, 123.17, 123.09, 121.83, 121.48, 121.44, 120.59, 119.27, 55.01, 44.14, 40.28, 32.16, 32.10, 32.09, 30.35, 30.01, 29.94, 29.91, 29.85, 29.63, 29.55, 29.53, 28.04, 26.72, 23.28, 23.25, 22.91, 22.85, 14.32, 14.27, 14.15, 14.11, 10.53.

FTIR (ATR, $CHCl_3$): υ (cm^{-1}): 2960, 2922, 2855, 2357, 1732, 1690, 1653, 1583, 1463, 1378, 1334, 1202, 1100.

MALDI-HRMS (*m/z*): calculated for $C_{104}H_{139}N_5O_2S_4$: 1617.9812, found (M^+): 1617.9782.

PIP-2TTP-DIA

Under Ar atmosphere, **PIP-2TTP (6)** (40 mg, 0.024 mmol) was dissolved in 1.5 mL of anhydrous chloroform and added to 5 mL of dry DMF solution. Then, the reaction was cooled down to 0 °C and $POCl_3$ (0.67 mL, 0.72 mmol) was added. After that, the reaction mixture was stirred at 0 °C for 2h and then heated to 90 ºC overnight. Once the time is over, the reaction was cooled and the crude was poured into NaOH 4M solution and extracted with dichloromethane (3 times). The combined organic phases were dried over $MgSO_4$ and, after removal of the solvent, purified by column chromatography in dichloromethane/hexane 4:1, to give **PIP-2TTP-DIA (8)** as a brown solid (32.6 mg, 81%).

^{1}H-NMR (300 MHz, $CDCl_3$): δ (ppm) = 10.15 (s, 2H), 8.35 (d, J = 7.9 Hz, 2H), 8.19-8.09 (m, 4H), 8.21 (d, J = 7.5 Hz, 2H), 4.86-4.74 (m, 4H), 3.67-3.59 (m, 2H), 3.22-3.08 (m, 4H), 2.44-2.33 (m, 2H), 2.00-1.89 (m, 4H), 1.82-1.73 (m, 1H), 1.27-0.95 (m, 82H), 0.89-0.68 (m, 30H).

FTIR (ATR, $CHCl_3$): υ (cm^{-1}): 2962, 2929, 2856, 2364, 1745, 1692, 1653, 1585, 1506, 1455, 1411, 1332, 1225, 1098.

MALDI-HRMS (*m/z*): calculated for $C_{106}H_{139}N_5O_4S_4$: 1673.9710, found (M^+): 1673.9705.

Y6-1Pery

Under Ar atmosphere, **PIP-2TTP-DIA (8)** (32.6 mg, 0.02 mmol) and 2-(3-oxo-2,3-dihydro-1H-inden-1-ylidene)malononitrile **9** (20 mg, 0.08 mmol) were suspended in 5 mL of dry chloroform and heated at 65 ºC until everything is dissolved. Then, pyridine (0.03 mL, 0.35 mmol) was added and stirred at 65 ºC overnight. Once the reaction time was over, the solvent was removed under reduced pressure ante the residue was purified by column chromatography in chloroform, to give the desired product **Y6-1Pery** as a purple solid (31 mg, 76%).

^{1}H-NMR (300 MHz, $CDCl_3$): δ (ppm) = 8.64 (s, 2H), 8.51-8.42 (m, 4H), 8.38-8.25 (m, 4H), 8.09-8.00 (m, 2H), 7.73-7.63 (m, 2H), 5.02-4.87 (m, 4H), 4.15-4.03 (m, 2H), 2.75-2.63 (m, 4H), 2.50-2.26 (m, 4H), 2.03-1.94 (m, 2H), 1.27-1.21 (m, 83H), 0.88-0.80 (m, 30H).

FTIR (ATR, $CHCl_3$): υ (cm^{-1}): 2956, 2916, 2855, 2340, 2218, 1695, 1662, 1586, 1555, 1533, 1419, 1348, 1281, 1228, 1208, 1142, 1095, 995, 888.

MALDI-HRMS (*m/z*): calculated for $C_{130}H_{143}F_4N_9O_4S_4$: 2098.0082, found ($M^+$): 2098.0165.

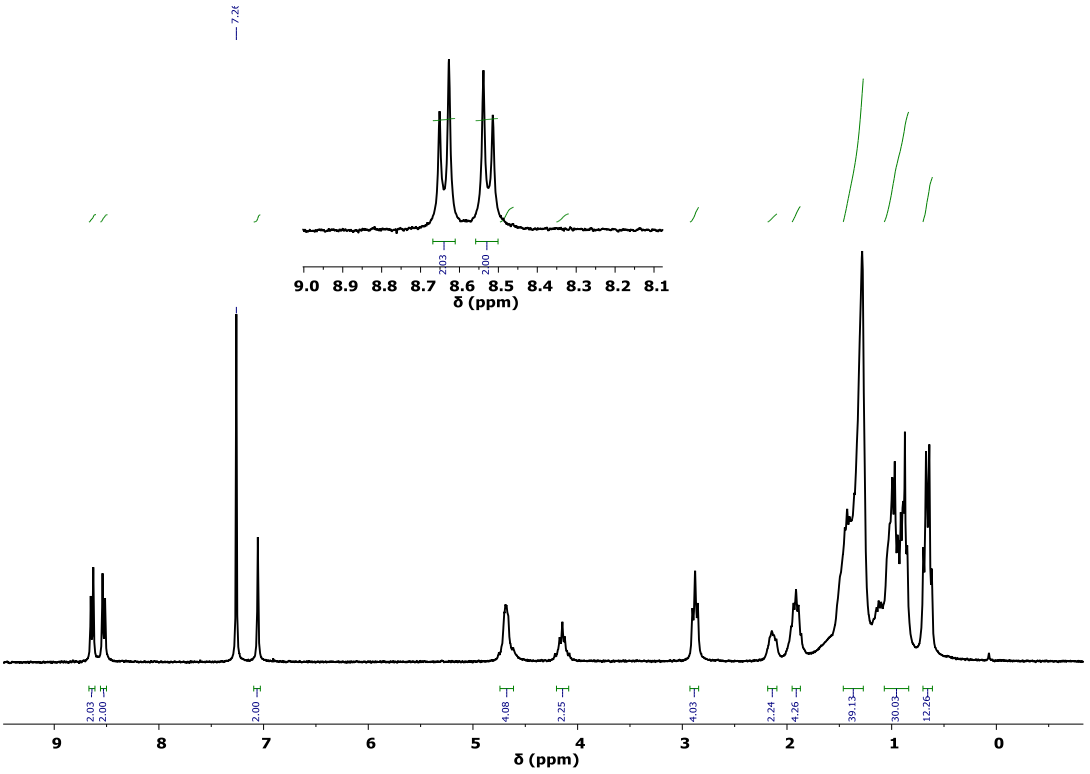

Figure S1. ^{1}H-NMR spectrum of **NIP-2TTP** in $CDCl_3$.

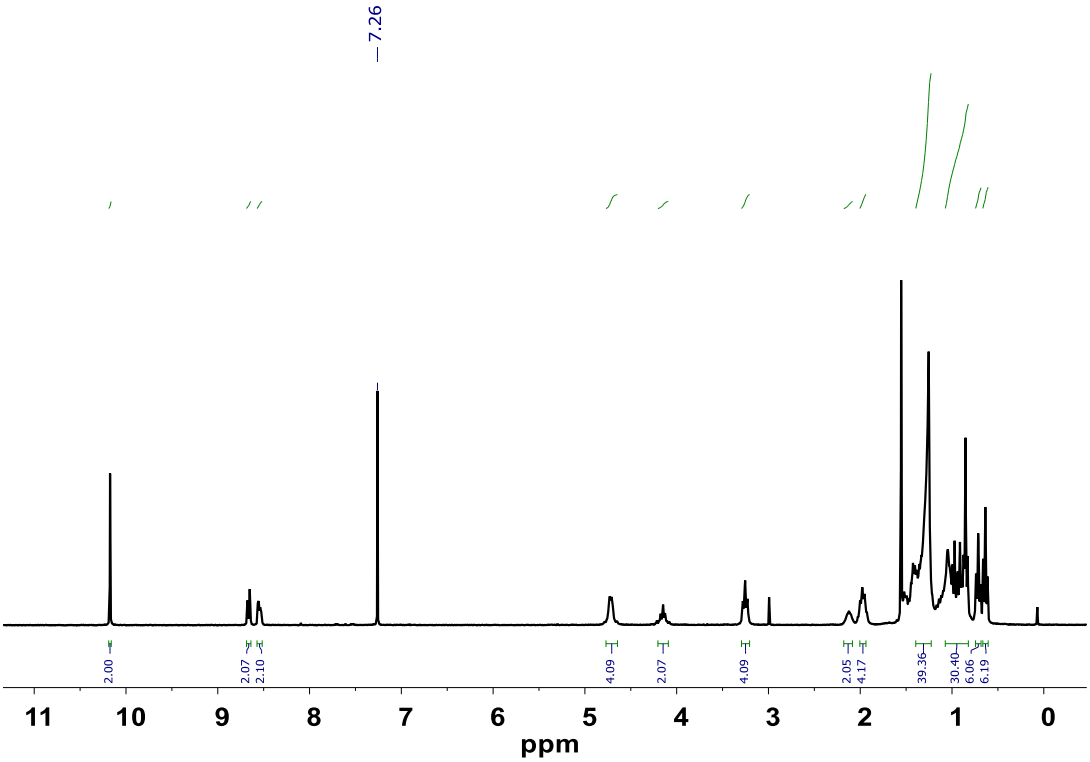

Figure S2. ^{1}H-NMR spectrum of **NIP-2TTP-DIA** in $CDCl_3$.

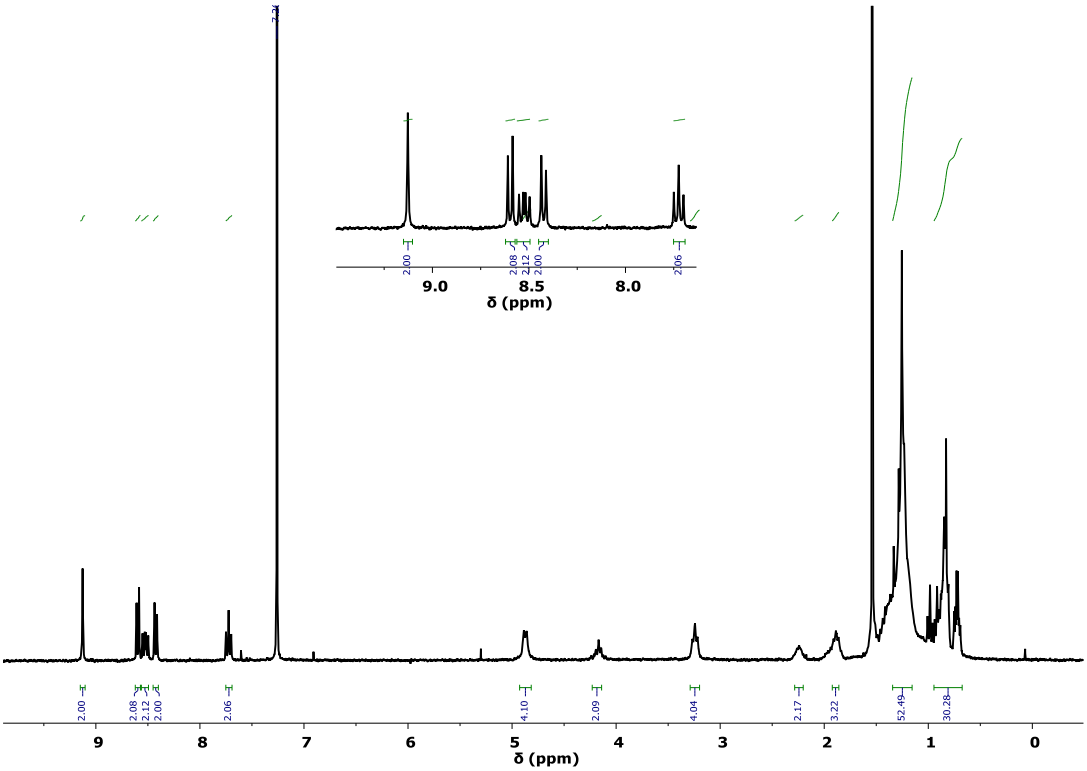

Figure S3. ^{1}H-NMR spectrum of **Y6-1Napht** in $CDCl_3$.

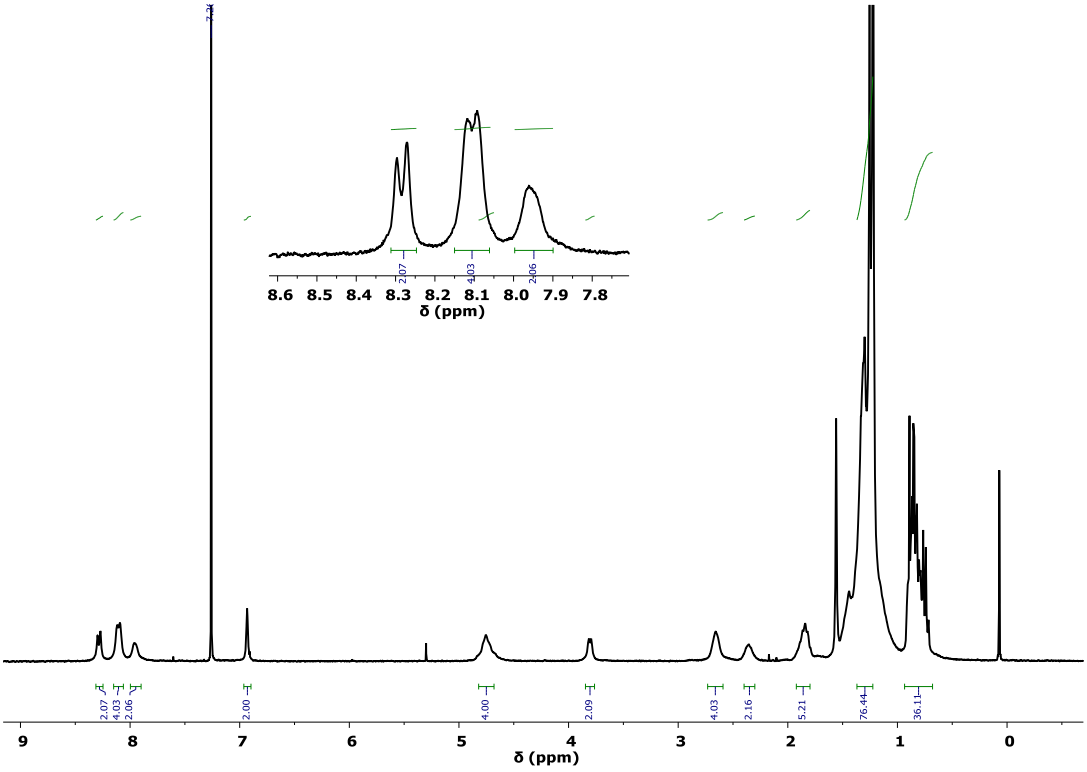

Figure S4. ^{1}H-NMR spectrum of **PIP-2TTP** in $CDCl_3$.

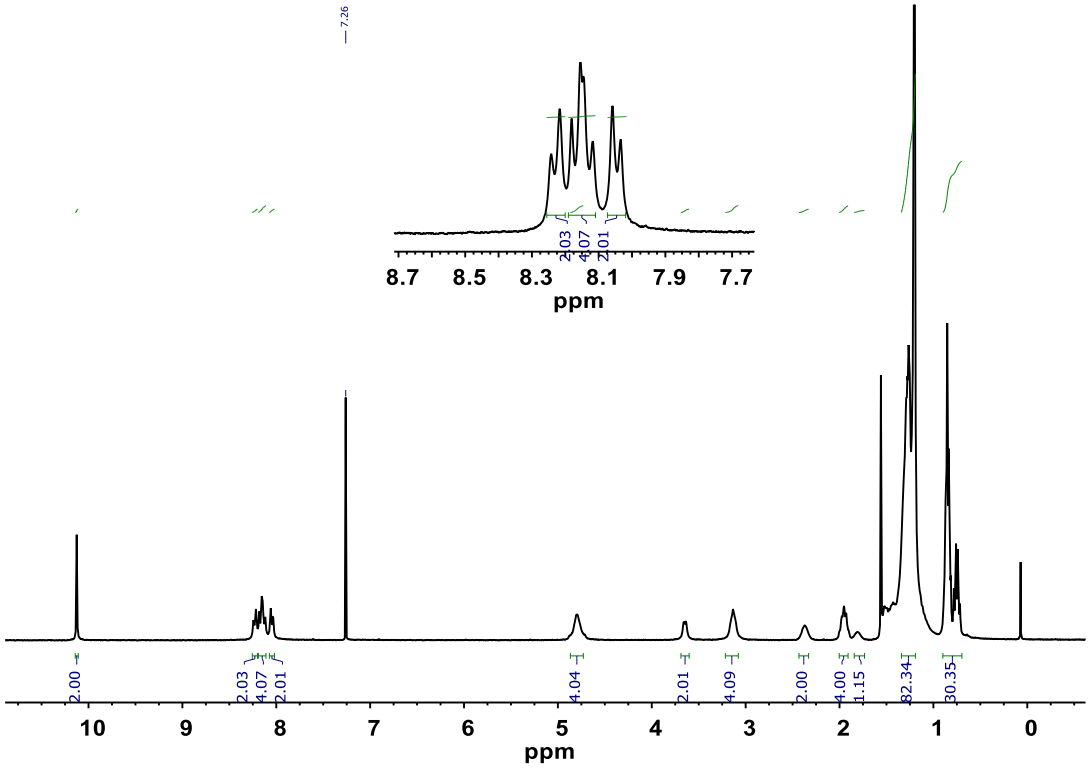

Figure S5. ^{1}H-NMR spectrum of **PIP-2TTP-DIA** in $CDCl_3$.

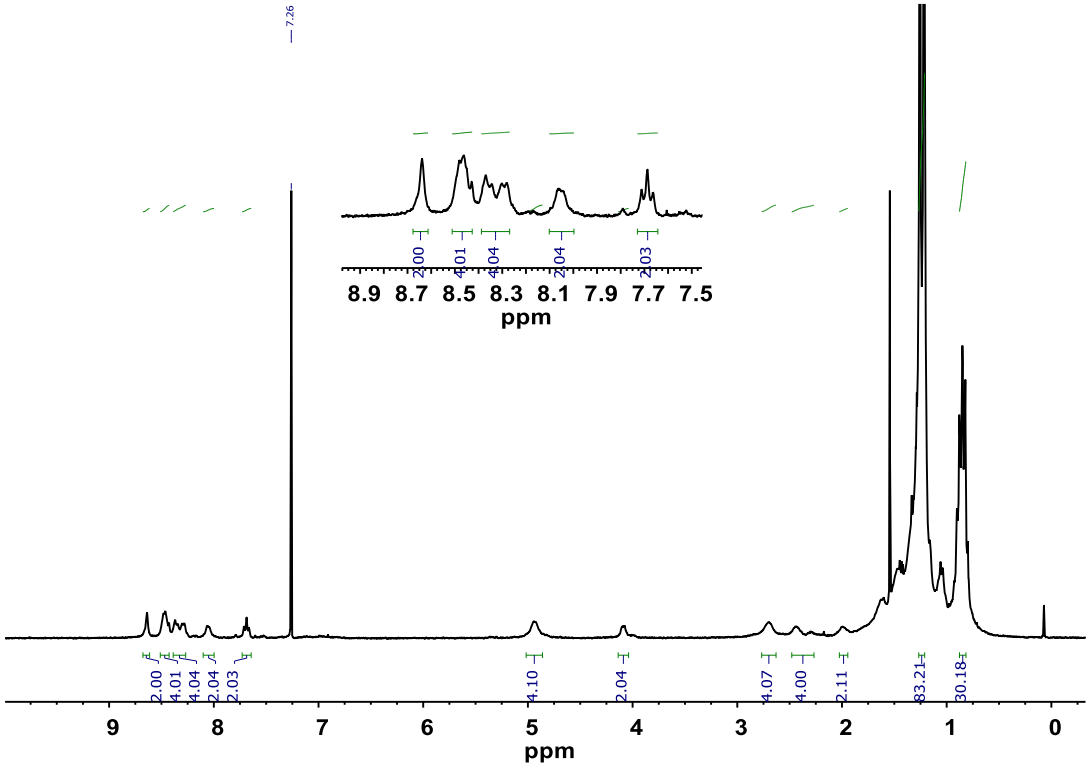

Figure S6. ^{1}H-NMR spectrum of **Y6-1Pery** in $CDCl_3$.

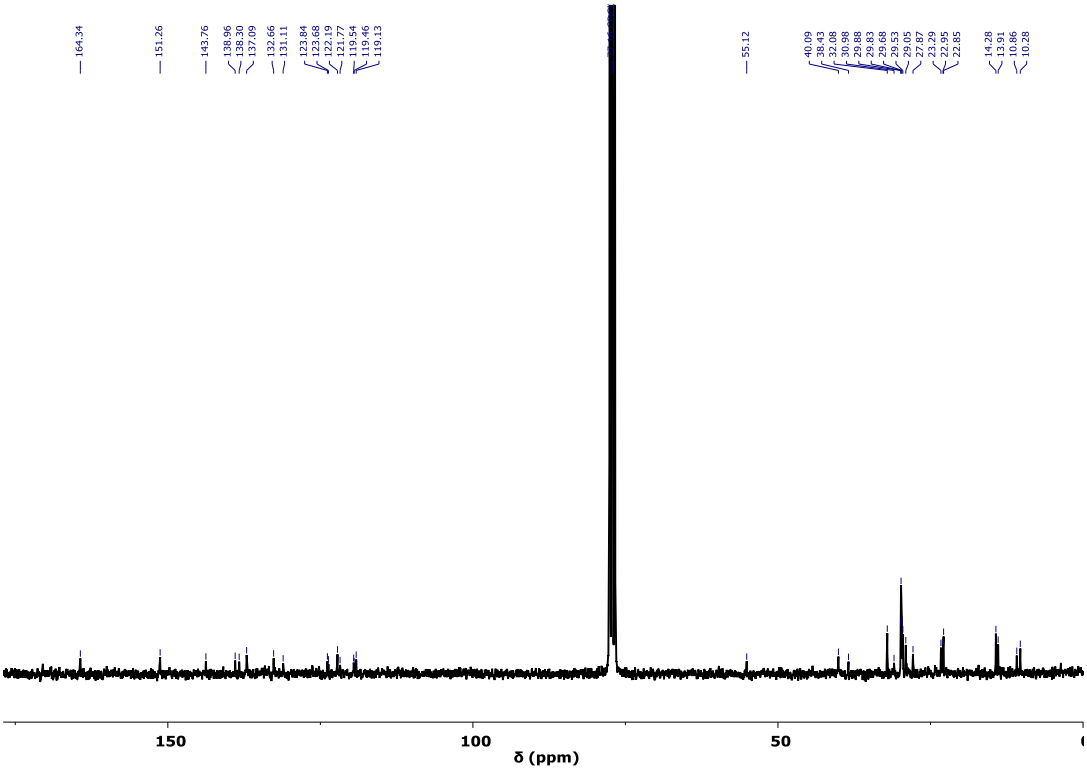

Figure S7. ^{13}C-NMR spectrum of **NIP-TTP** in $CDCl_3$.

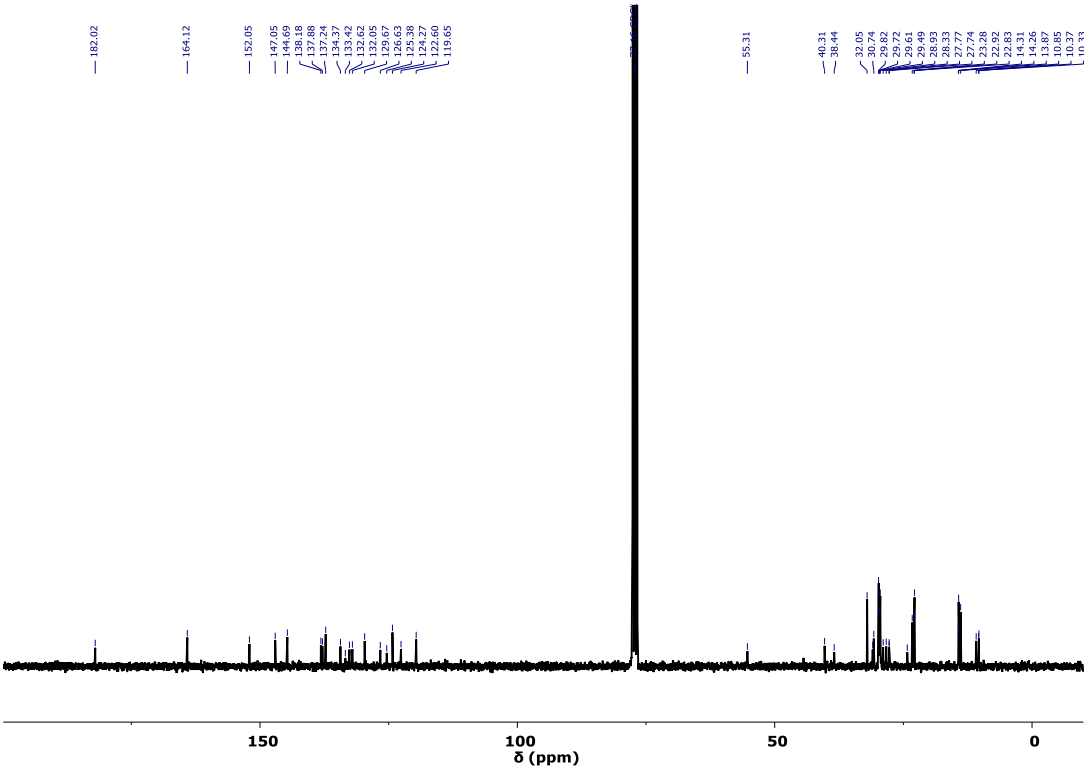

Figure S8. ^{13}C-NMR spectrum of **NIP-2TTP-DIA** in $CDCl_3$.

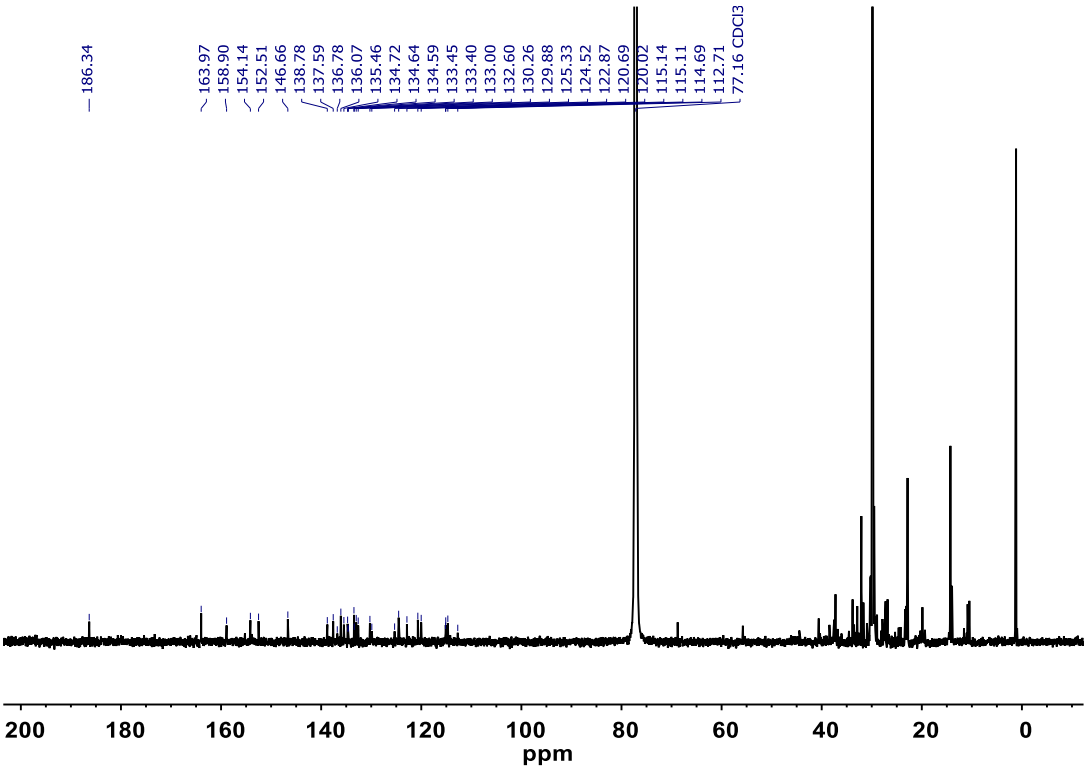

Figure S9. ^{13}C-NMR spectrum of **Y6-1Napht** in $CDCl_3$ (175 MHz).

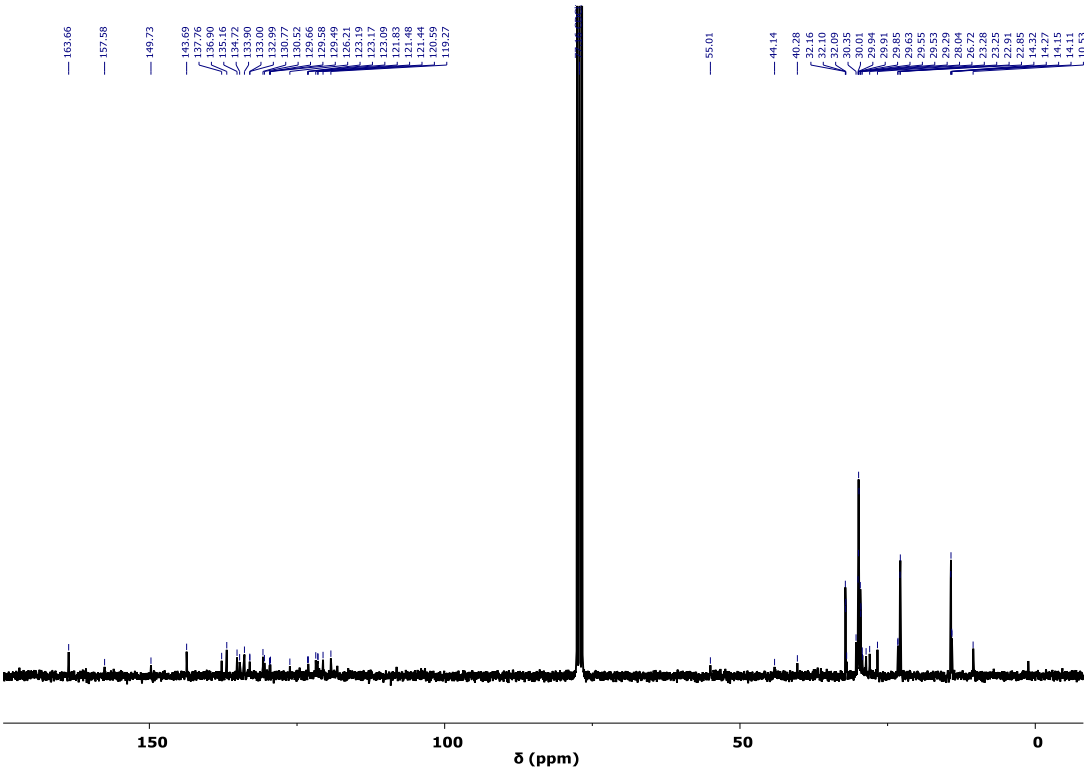

Figure S10. ^{13}C-NMR spectrum of **PIP-2TTP** in $CDCl_3$.

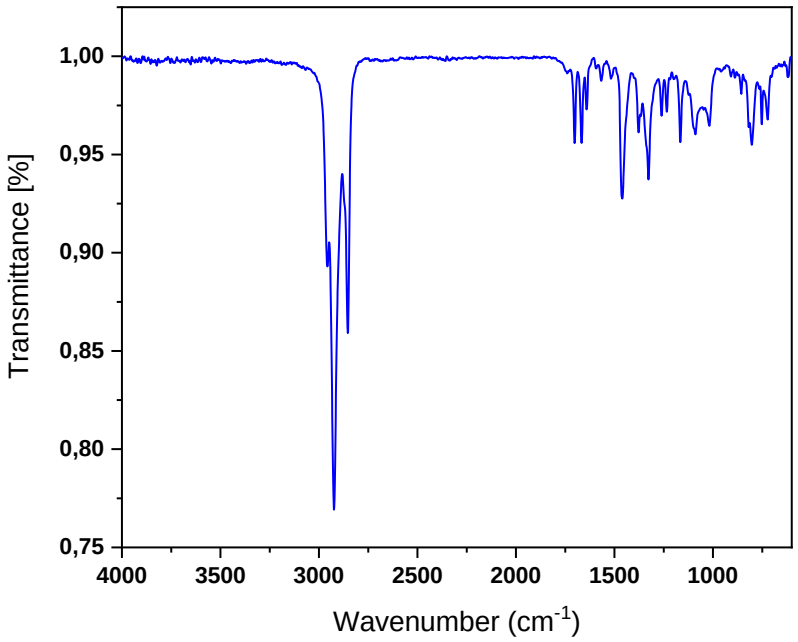

Figure S11. IR spectrum of **NIP-2TTP**.

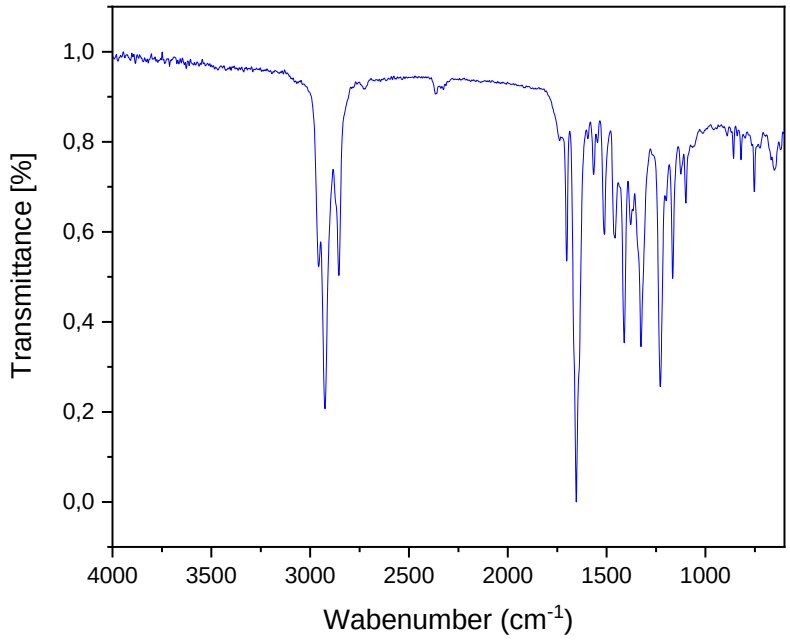

Figure S12. IR spectrum of **NIP-2TTP-DIA**.

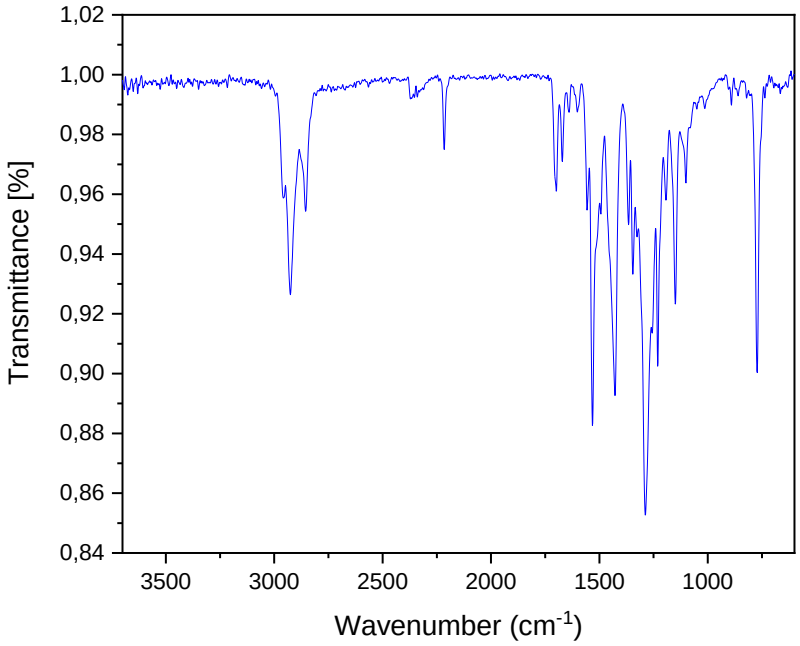

Figure S13. IR spectrum of **Y6-1Napht**.

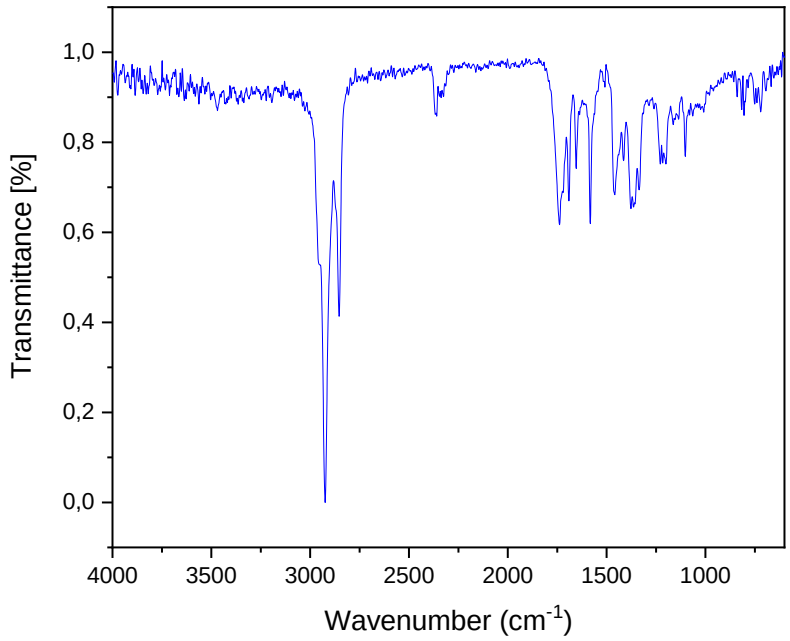

Figure S14. IR spectrum of **PIP-2TTP**.

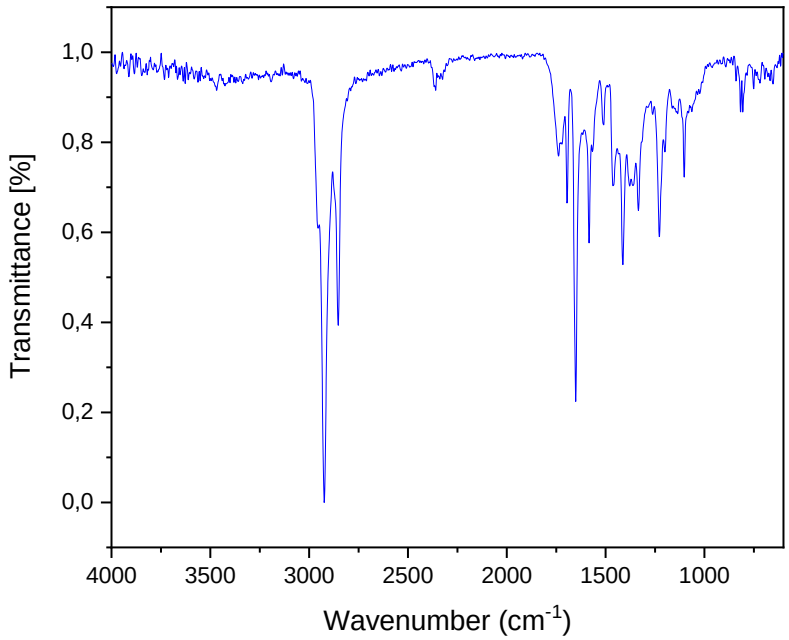

Figure S15. IR spectrum of **PIP-2TTP-DIA**.

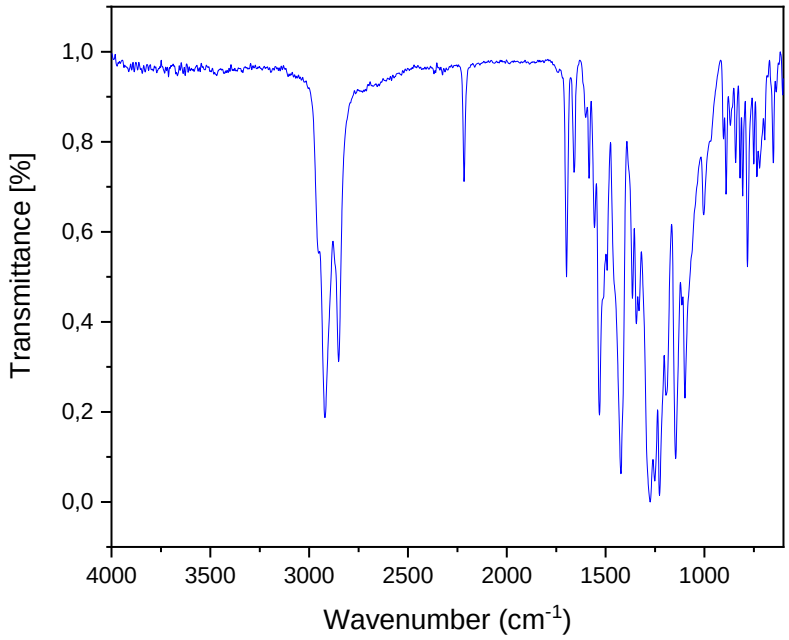

Figure S16. IR spectrum of **Y6-1Pery**.

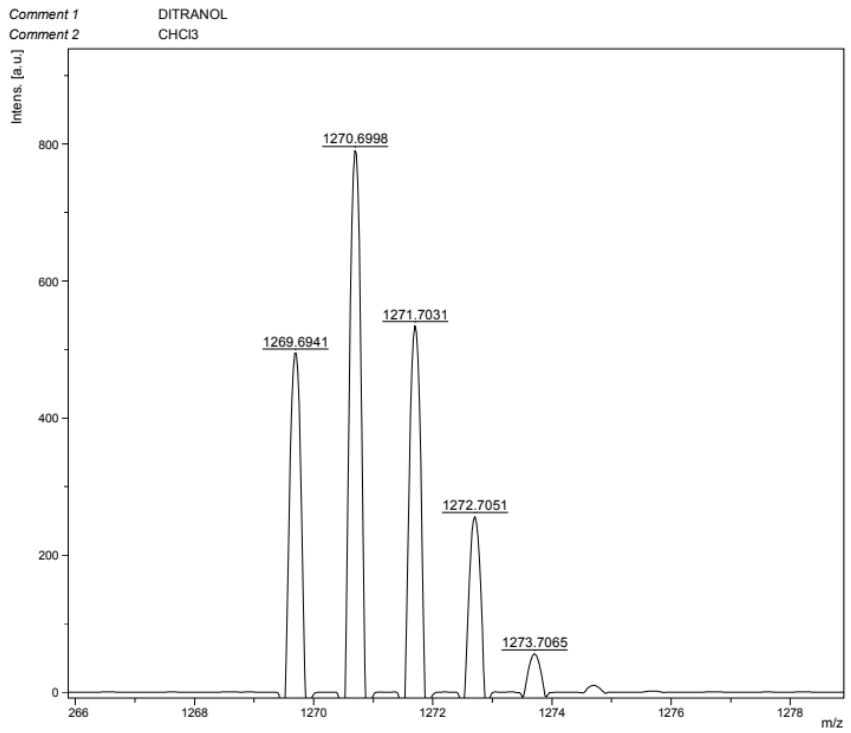

Figure S17. MALDI-HRMS (m/z) spectrum of **NIP-2TTP**.

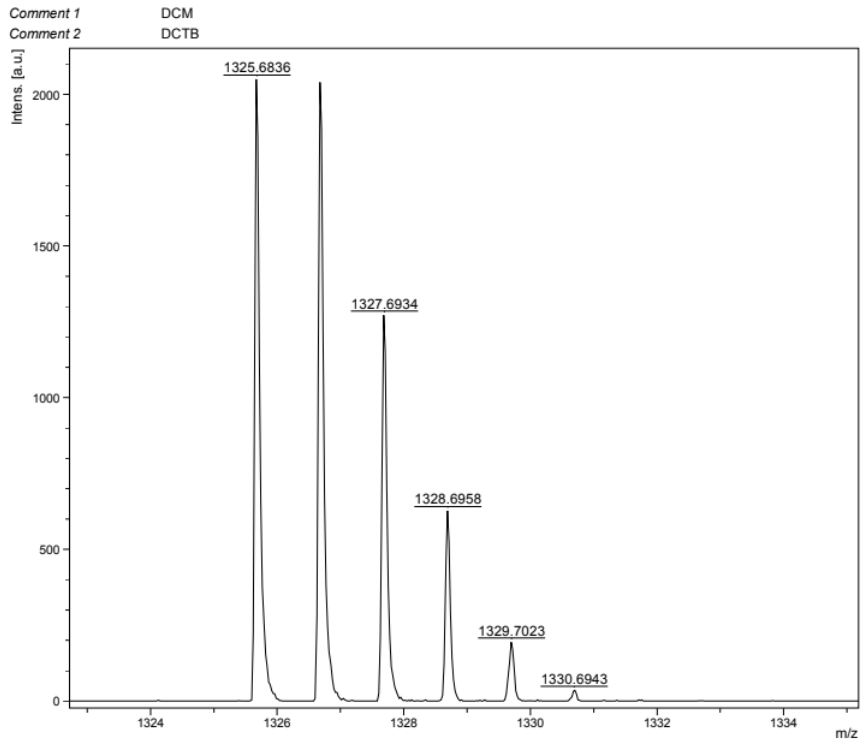

Figure S18. MALDI-HRMS (m/z) spectrum of **NIP-2TTP-DIA.**

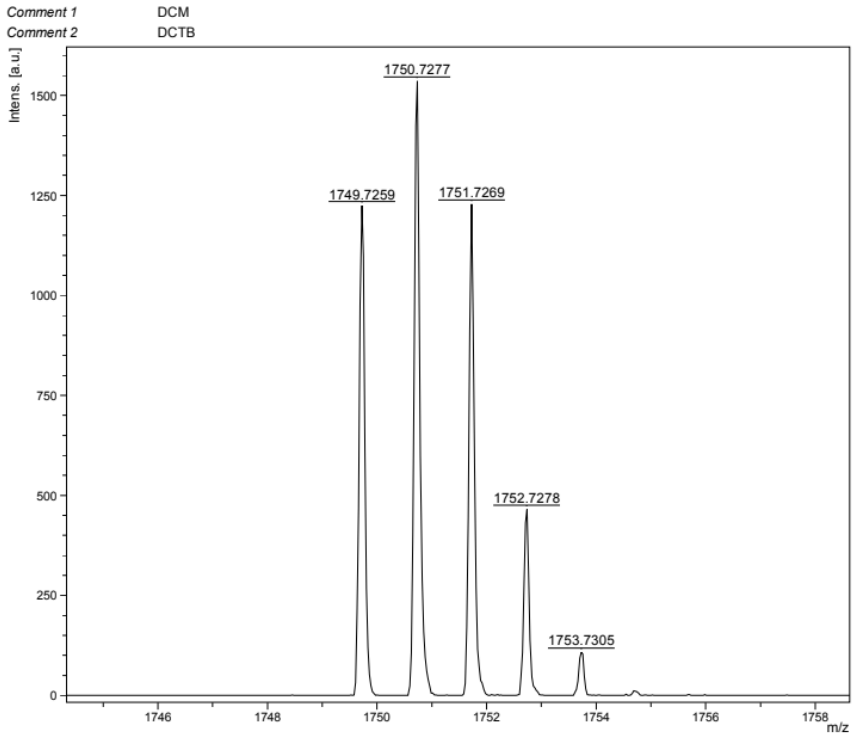

Figure S19. MALDI-HRMS (m/z) spectrum of **Y6-1Napht.**

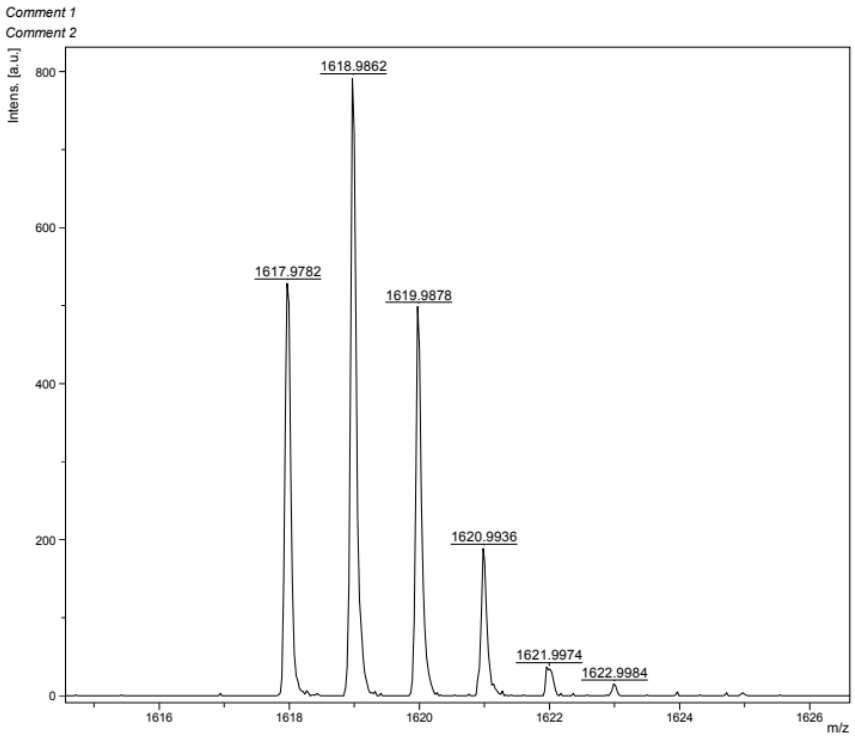

Figure S20. MALDI-HRMS (m/z) spectrum of **PIP-2TTP.**

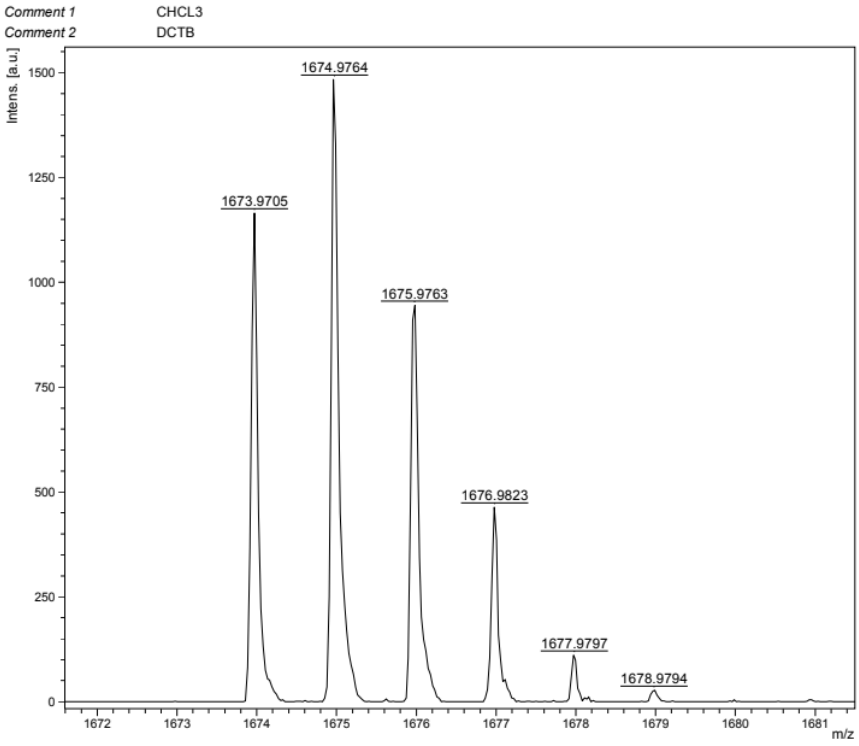

Figure S21. MALDI-HRMS (m/z) spectrum of **PIP-2TTP-DIA.**

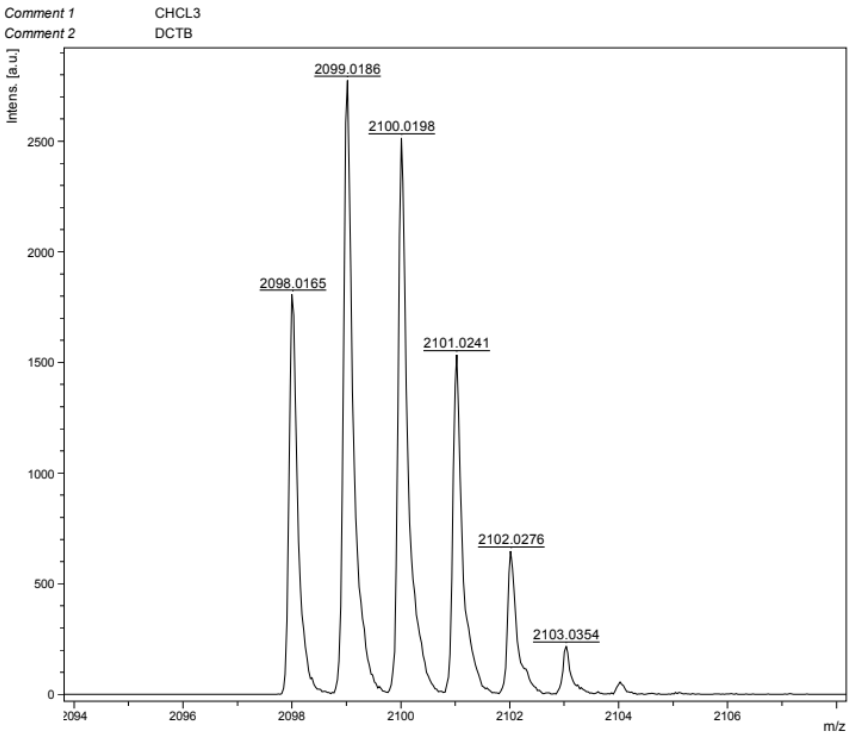

Figure S22. MALDI-HRMS (m/z) spectrum of **Y6-1Pery.**

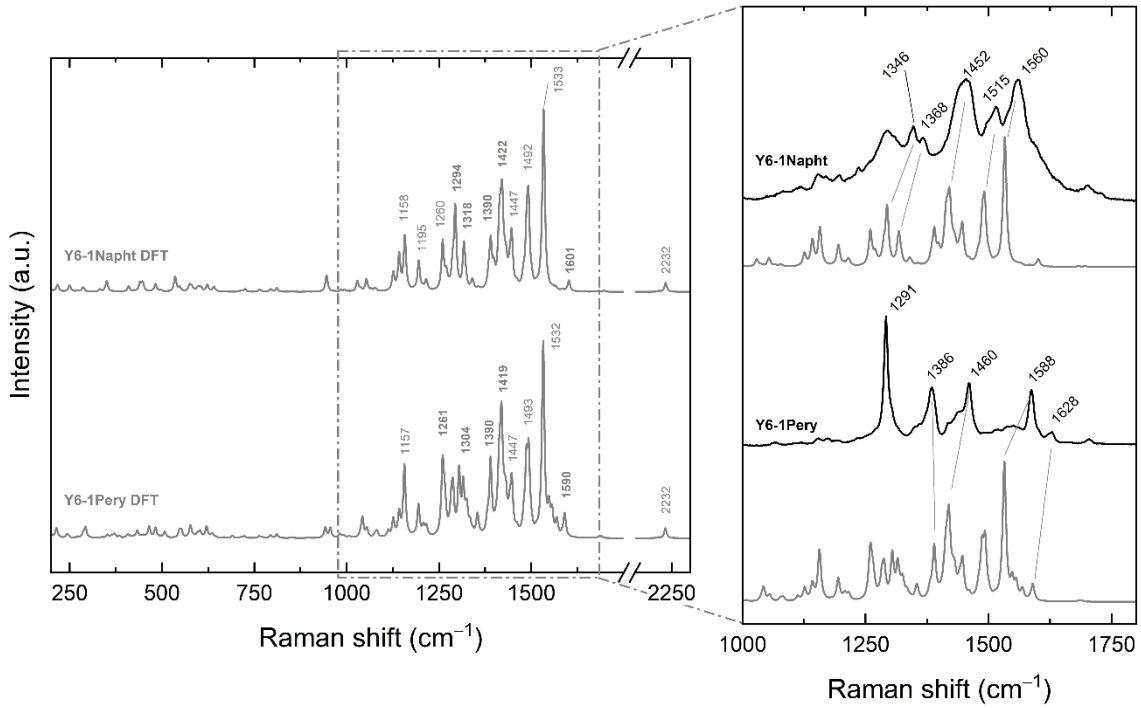

Figure S23. Gas-phase DFT simulated Raman spectra of Y6 derivatives intramolecular modes (200-2300 cm^{-1}). The pending C_8 alkyl chains were removed to simplify the calculations. Reference vibrations are highlighted for each molecule. In the close up, the comparison between the experimental spectra (black) and the simulated ones (grey) of the Y6 derivatives.

Table S1. Simulated wavenumbers of the Y6 derivatives compared to the experimental ones.

	Y6-1Napht		**Y6-1Pery**	
mode	**calc**	**exp**	**calc**	**exp**
ν(C≡N)	2232	–	2232	–
ν(C=C) Napht-head	1601	–	–	–
ν(C=C) Pery-head	–	–	1590	1628
ν(C=C) central aromatic rings	1533	1560	1532	1588
ν(C=C–N)	1492	1515	1493	–
δ(CH_3)	1447	–	1447	–
ν(C=C–CH, N–CH_3) Napht-head	1422	1452	1419	1460
δ(CH_3) terminal	1390	–	1390	1386
ν(C=C–N–CH_3) central arom. rings	1318	1368	–	–
ν(C=C) Pery-head	–	–	1304	–
ν(N–C=C–N) central bond	1294	1346	–	–
ρ(CH) terminal Pery-head	–	–	1261	–

ν(C=C) conjugated Y6 core	1260	–	–	–
ρ(N–CH_3) terminal alkyl groups	1195	–	–	–
ν(CC) central ring, ρ(CH_3) terminal	1158	–	1157	–

3. UV-Vis, emission and electrochemical data.

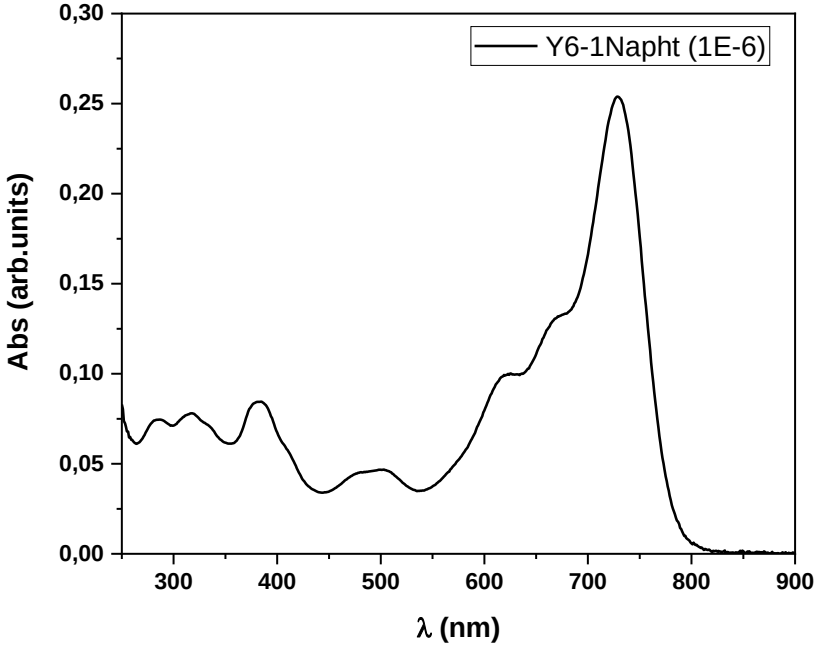

Figure S24. UV-Vis spectra of **Y6-1Napht** 1.0×10^{-6} M in chloroform solution.

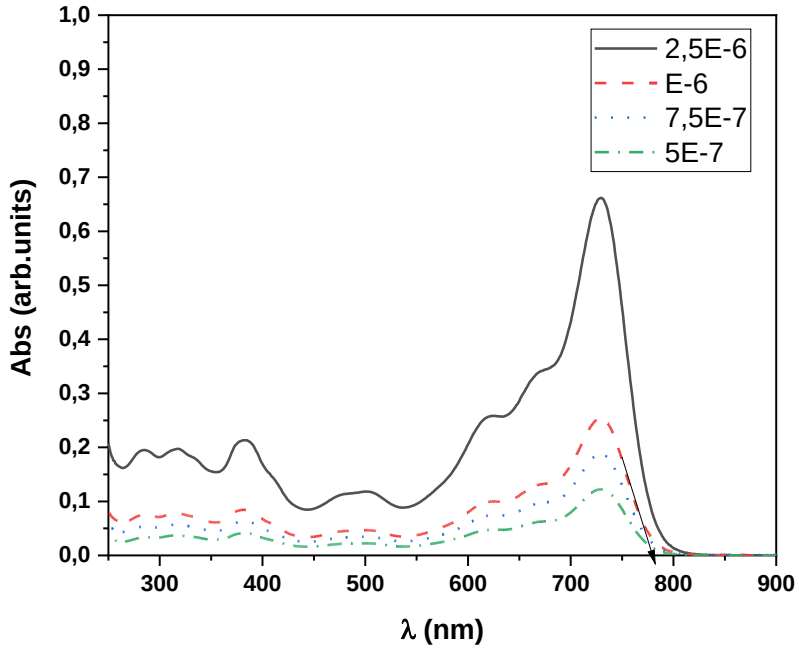

Figure S25. UV-Vis spectrum of **Y6-1Napht** dilutions in chloroform solution.

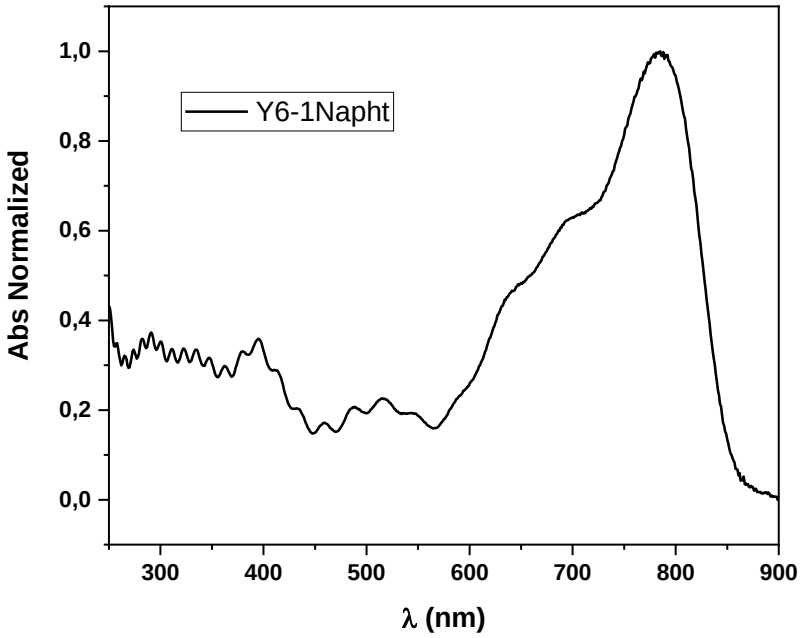

Figure S26. UV-Vis spectrum of **Y6-1Napht** in film.

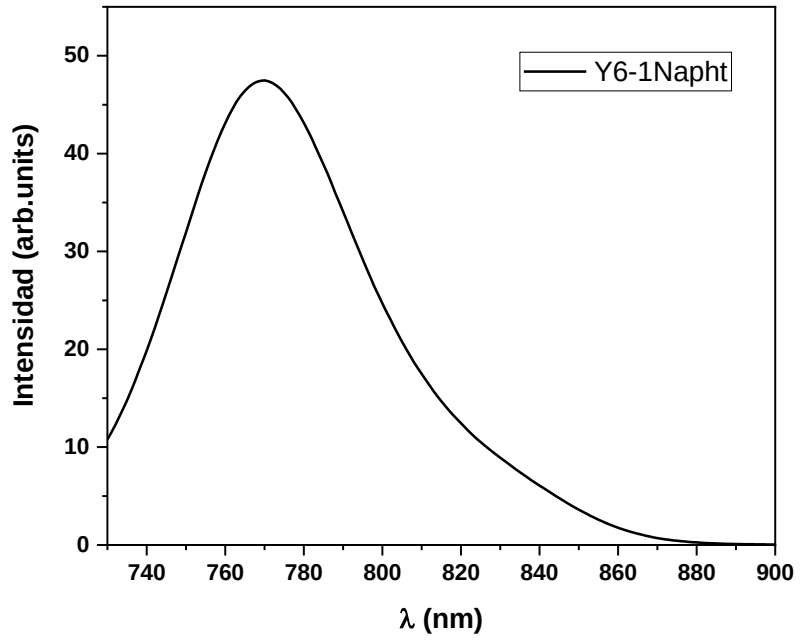

Figure S27. Emission spectra of **Y6-1Napht** 1.0×10^{-6} M in chloroform solution.

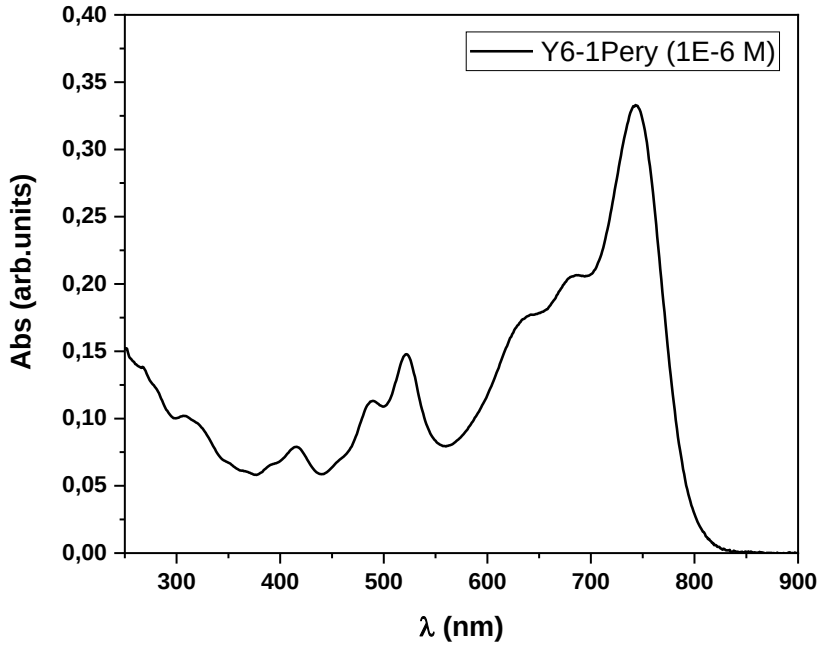

Figure S28. UV-Vis spectra of **Y6-1Pery** 1.0×10^{-6} M in chloroform solution.

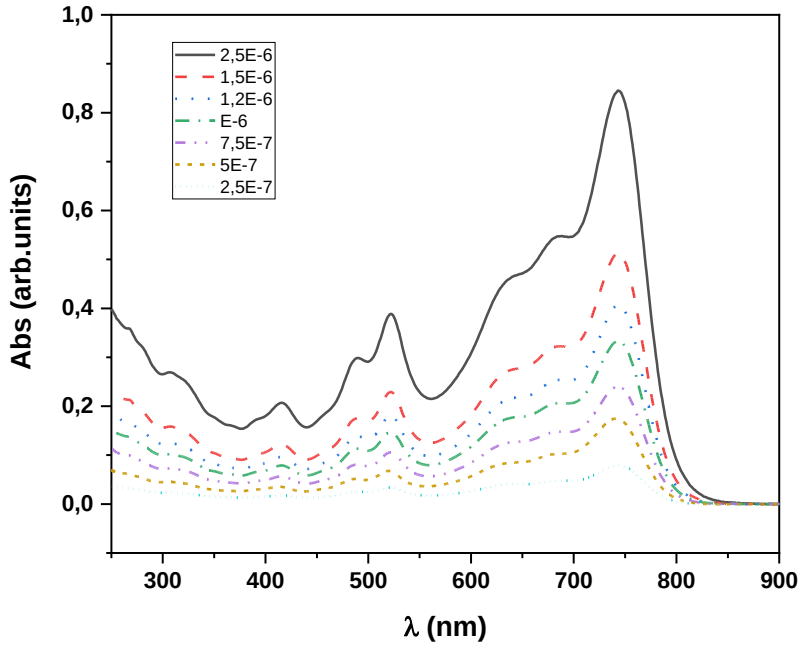

Figure S29. UV-Vis spectrum of **Y6-1Pery** dilutions in chloroform solution.

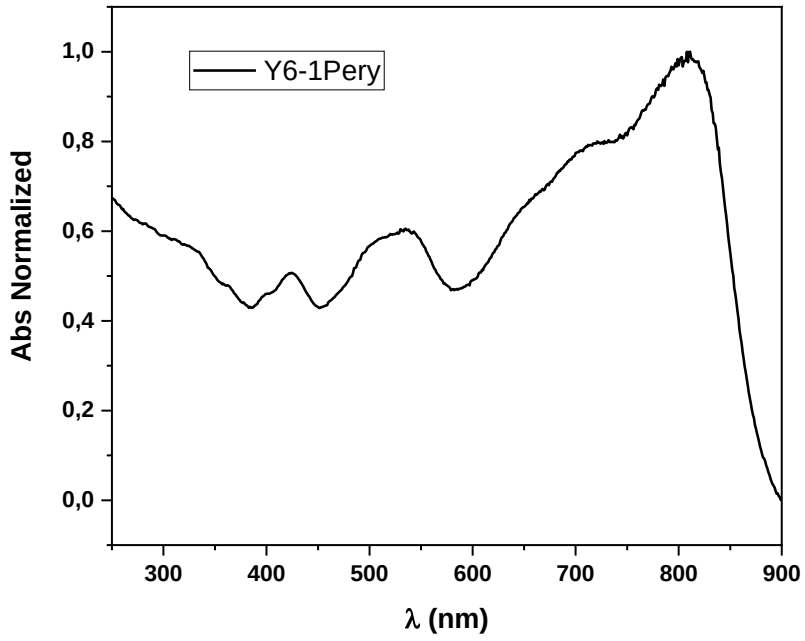

Figure S30. UV-Vis spectra of **Y6-1Pery** in film.

Table S2. Comparison between the theoretical and experimental absorption properties for **Y6**, **Y6-1Napht** and **Y6-1Pery**.

	λ_{max} (nm)		Electronic transitions
molecule	**calc**	**exp**	
Y6	683	731	HOMO → LUMO
Y6-1Napht	674	730	HOMO → LUMO
Y6-1Pery	695	743	HOMO → LUMO

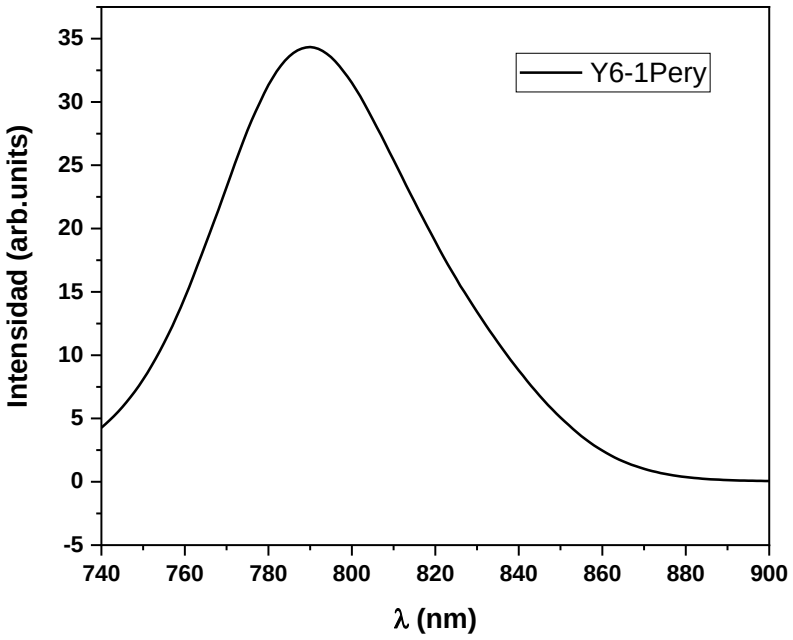

Figure S31. Emission spectra of **Y6-1Pery** 1.0×10^{-6} M in chloroform solution.

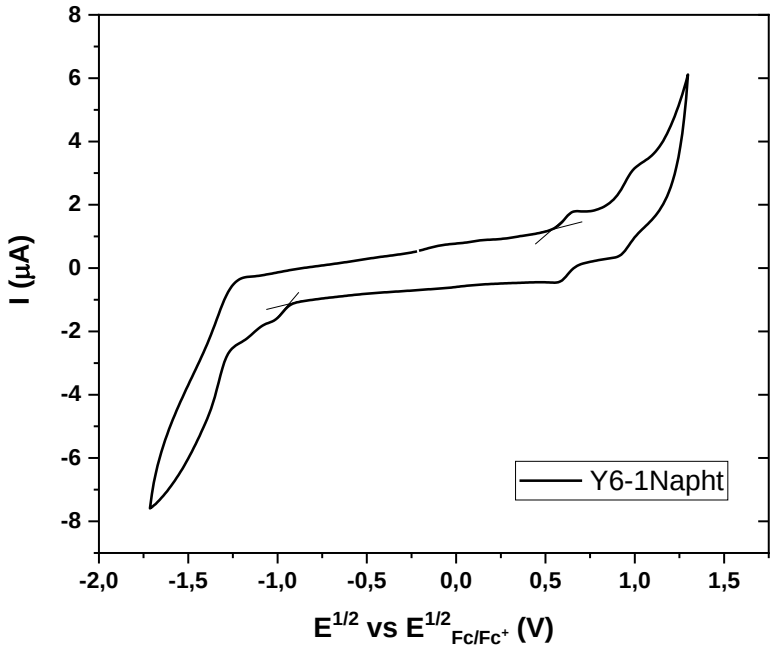

Figure S32. Cyclic voltammetry spectrum of **Y6-1Napht**.

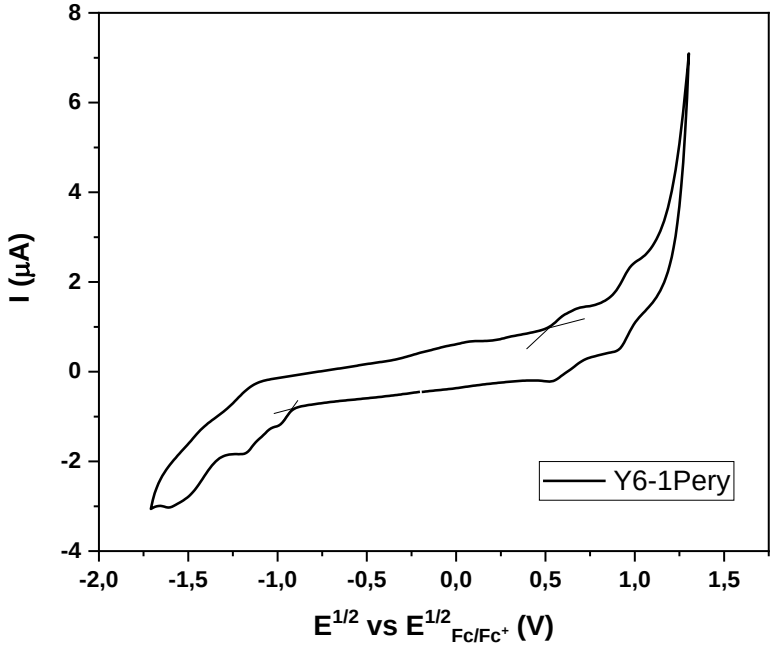

Figure S33. Cyclic voltammetry spectrum of **Y6-1Pery**.

4. Thermal and microscopic analysis.

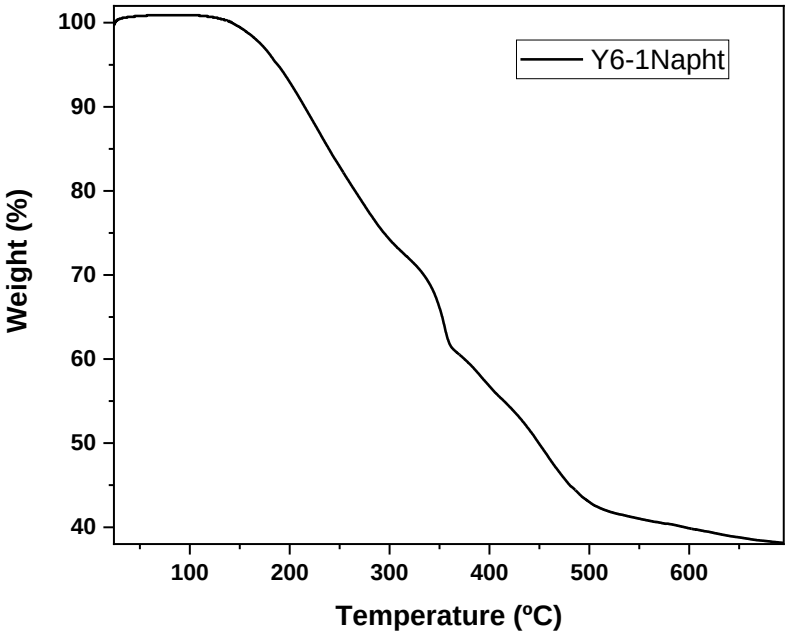

Figure S34. Thermogravimetric analysis of **Y6-1Napht**.

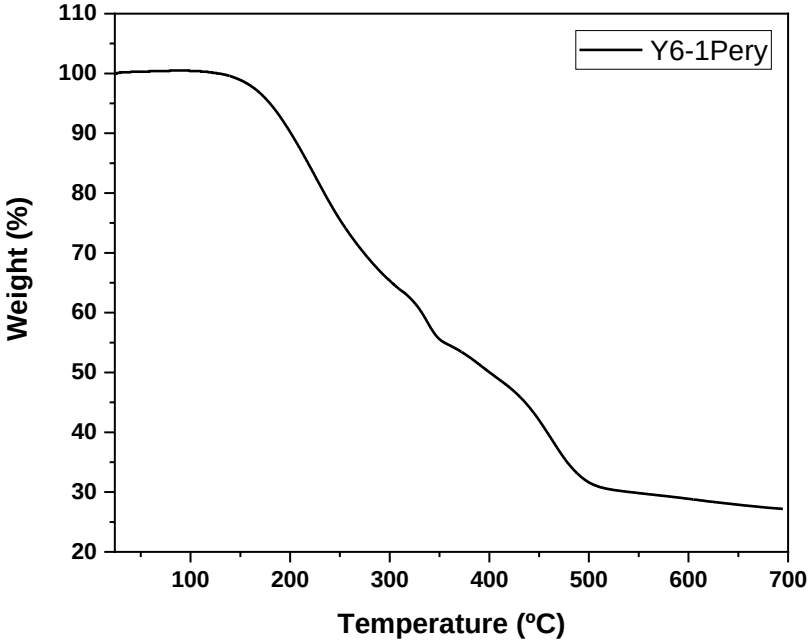

Figure S35. Thermogravimetric analysis of **Y6-1Pery**.

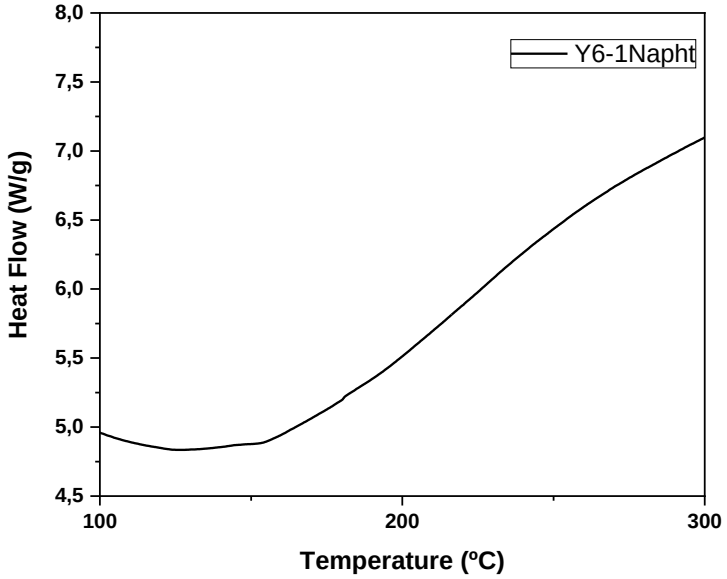

Figure S36. Differential scanning calorimetry analyses of **Y6-1Napht.**

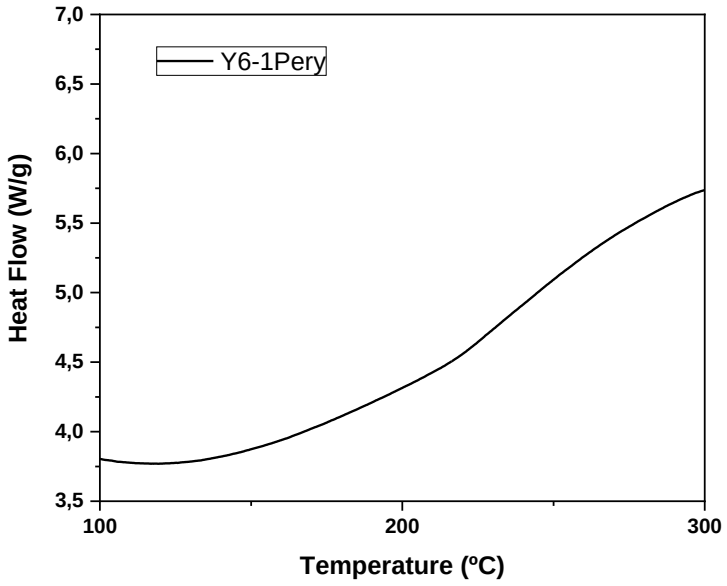

Figure S37. Differential scanning calorimetry analyses of **Y6-1Pery.**

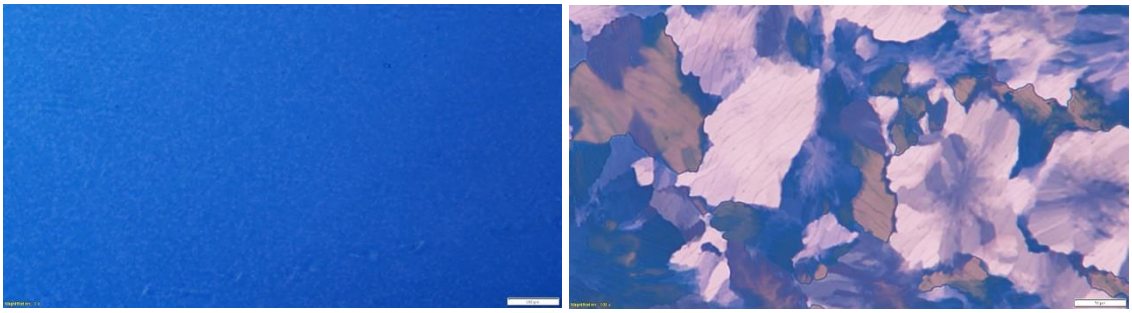

Figure S38. Left) Microscope image of **Y6** thin film annealed at 180 ºC (scale bar 200 µm). **Right)** Microscope image of **Y6** thin film annealed at 250 ºC (scale bar 10 µm).

5. OSC results.

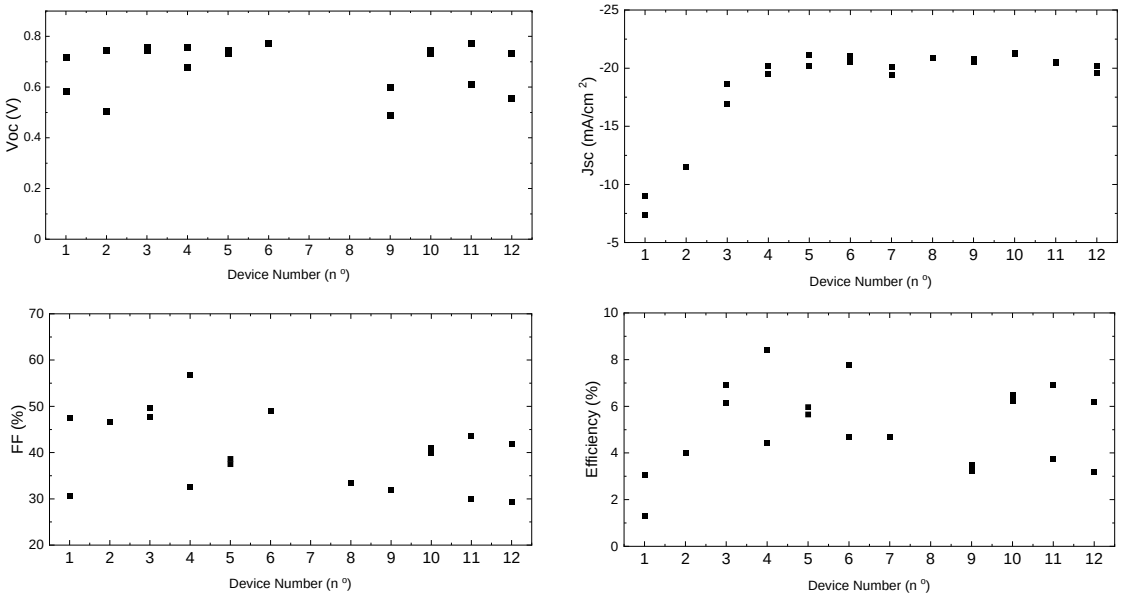

Figure S39. Main photovoltaic parameters of **Y6**:**PM6** blade coated solar cells as a function of active layer thickness. The data shown correspond to a single substrate in which the active layer has deposited with a thickness gradient, so each pixel exhibits a slightly different thickness. Device number is a proxy for thickness, in which 1 is the thinnest layer and 12 the thicker layer.

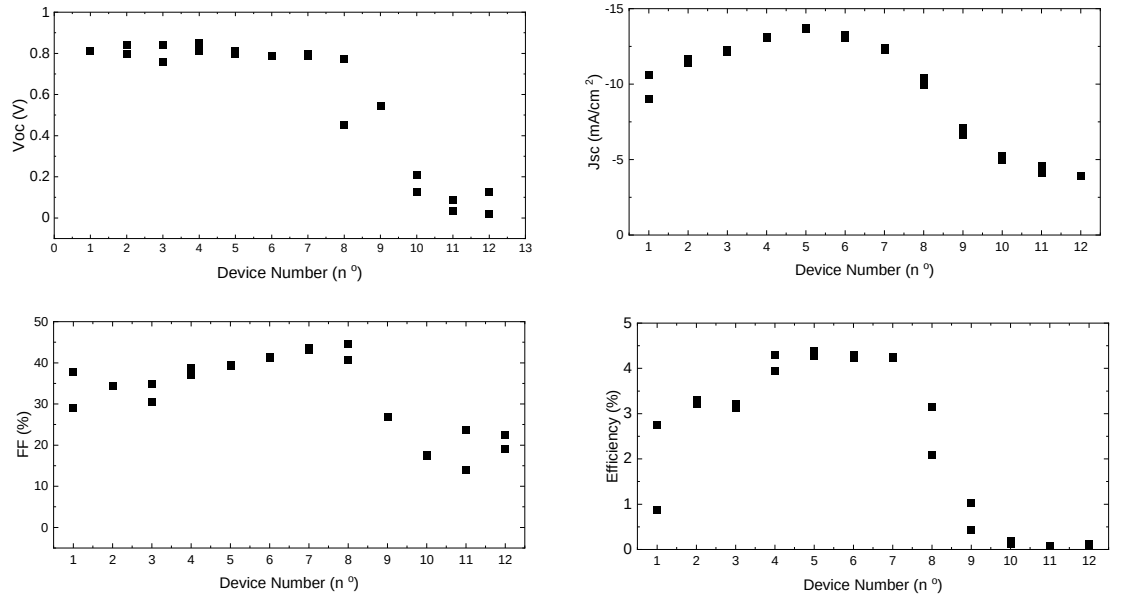

Figure S40. Main photovoltaic parameters of **Y6-1Pery:PM6** blade coated solar cells as a function of active layer thickness. Device number is a proxy where 1 is the thinnest layer and 12 the thicker layer.

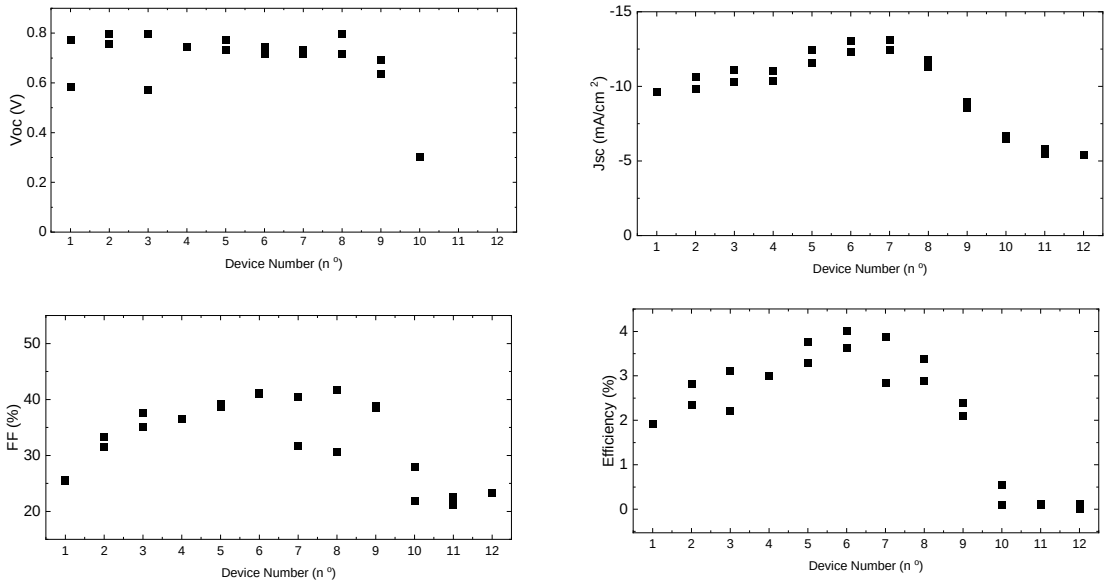

Figure S41. Main photovoltaic parameters of **Y6-1Napht:PM6** blade coated solar cells as a function of active layer thickness. Device number is a proxy where 1 is the thinnest layer and 12 the thicker layer.

6. References.

[1] a) J. Yuan, Y. Zhang, L. Zhou, G. Zhang, H.-L. Yip, T.-K. Lau, X. Lu, C. Zhu, H. Peng, P. A. Johnson, M. Leclerc, Y. Cao, J. Ulanski, Y. Li, Y. Zou, *Joule* **2019**, *3*, 1140-1151; b) H. Herrera, P. de Echegaray, M. Urdanpilleta, M. J. Mancheño, E. Mena-Osteritz, P. Bäuerle, J. L. Segura, *Chemical Communications* **2013**, *49*, 713-715; c) P. de Echegaray, M. J. Mancheño, I. Arrechea-Marcos, R. Juárez, G. López-Espejo, J. T. López Navarrete, M. M. Ramos, C. Seoane, R. P. Ortiz, J. L. Segura, *The Journal of Organic Chemistry* **2016**, *81*, 11256-11267; d) M. J. Alonso-Navarro, A. Harbuzaru, P. de Echegaray, I. Arrechea-Marcos, A. Harillo-Baños, A. de la Peña, M. M. Ramos, J. T. López Navarrete, M. Campoy-Quiles, R. Ponce Ortiz, J. L. Segura, *Journal of Materials Chemistry C* **2020**, *8*, 15277-15289.

[2] A. D. Becke, *The Journal of Chemical Physics* **1993**, *98*, 5648-5652.

[3] L. A. Curtiss, M. P. McGrath, J. P. Blaudeau, N. E. Davis, R. C. Binning, Jr., L. Radom, *The Journal of Chemical Physics* **1995**, *103*, 6104-6113.

[4] H. B. S. G. W. S. M. J. T. Frisch, G. E.; Robb, M. A.; Cheeseman, J. R.; Scalmani, G.; Barone, V.; Petersson, G. A.; Nakatsuji, H.; Li, X.; Caricato, M.; Marenich, A. V.; Bloino, J.; Janesko, B. G.; Gomperts, R.; Mennucci, B.; Hratchian, H. P.; Ortiz, J. V.; Izmaylov, A. F.; Sonnenberg, J. L.; Williams-Young, D.; Ding, F.; Lipparini, F.; Egidi, F.; Goings, J.; Peng, B.; Petrone, A.; Henderson, T.; Ranasinghe, D.; Zakrzewski, V. G.; Gao, J.; Rega, N.; Zheng, G.; Liang, W.; Hada, M.; Ehara, M.; Toyota, K.; Fukuda, R.; Hasegawa, J.; Ishida, M.; Nakajima, T.; Honda, Y.; Kitao, O.; Nakai, H.; Vreven, T.; Throssell, K.; Montgomery, J. A., Jr.; Peralta, J. E.; Ogliaro, F.; Bearpark, M. J.; Heyd, J. J.; Brothers, E. N.; Kudin, K. N.; Staroverov, V. N.; Keith, T. A.; Kobayashi, R.; Normand, J.; Raghavachari, K.; Rendell, A. P.; Burant, J. C.; Iyengar, S. S.; Tomasi, J.; Cossi, M.; Millam, J. M.; Klene, M.; Adamo, C.; Cammi, R.; Ochterski, J. W.; Martin, R. L.; Morokuma, K.; Farkas, O.; Foresman, J. B.; Fox, D. J., **2016**.

[5] a) E. Runge, E. K. U. Gross, *Physical Review Letters* **1984**, *52*, 997-1000; b) M. Petersilka, U. J. Gossmann, E. K. U. Gross, *Physical Review Letters* **1996**, *76*, 1212-1215; c) M. E. Casida, C. Jamorski, K. C. Casida, D. R. Salahub, *The Journal of Chemical Physics* **1998**, *108*, 4439-4449.

[6] M. Malagoli, J. Brédas, *Chemical Physics Letters - CHEM PHYS LETT* **2000**, *327*, 13-17.